

Organizacija mikrotubula i ravnoteža sila u metafaznom vretenu HeLa i Ptk1 stanica

Vukušić, Kruno

Master's thesis / Diplomski rad

2015

Degree Grantor / Ustanova koja je dodijelila akademski / stručni stupanj: **University of Zagreb, Faculty of Science / Sveučilište u Zagrebu, Prirodoslovno-matematički fakultet**

Permanent link / Trajna poveznica: <https://urn.nsk.hr/urn:nbn:hr:217:764212>

Rights / Prava: [In copyright](#) / [Zaštićeno autorskim pravom.](#)

Download date / Datum preuzimanja: **2024-04-19**



Repository / Repozitorij:

[Repository of the Faculty of Science - University of Zagreb](#)



University of Zagreb
Faculty of Science
Department of Biology

Kruno Vukušić

**Organisation of microtubules and force-balance in
metaphase spindles of HeLa and Ptk1 cells**

Graduation Thesis

Zagreb, 2015.

Work for this thesis was done at Ruđer Bošković Institute in Laboratory for Electron Microscopy on Division of Molecular Biology, under supervisorship of Dr. Iva Tolić, Prof. (Laboratory for Electron Microscopy, Division of Molecular Biology, Ruđer Bošković Institute, 10000 Zagreb, Croatia). Cosupervisor was Dr. Biljana Balen, Assoc. Prof. (Division of Molecular Biology, Department of Biology, Faculty of Science, University of Zagreb, 10000 Zagreb, Croatia). Thesis was submitted for evaluation to Department of Biology, Faculty of Science, University of Zagreb to achieve the academic degree Master of Molecular Biology (mag. biol. mol.).

Acknowledgments

I would like to give special thanks to: Iva Tolić, for being great group leader, for opportunity to work as part of this project and for broadening my scientific perception; Ivana Šarić for introducing me to Adobe Illustrator and for drawing some of the graphs; Biljana Balen for reviewing this thesis; Renata Buđa for being excellent lab partner in good and bad times; Bruno Polak for very nice introduction in cell culture procedures; Ana Milas for enduring my continuous late night e-mails, for introduction to Fiji and for work done in MatLab; members of Nenad Pavin group for showing to me how molecular biology can be combined with theoretical physics; my parents, sisters, relatives and friends from Dalmatia for their constant support through my entire life and education and my girlfriend Željka for enduring my long monologs about this project and for many nice moments in last seven years.

TEMELJNA DOKUMENTACIJSKA KARTICA

Sveučilište u Zagrebu
Prirodoslovno-matematički fakultet
Biološki odsjek

Diplomski rad

Organizacija mikrotubula i ravnoteža sila u metafaznom vretenu HeLa i Ptk1 stanica

Kruno Vukušić

Rooseveltov trg 6, 10000, Zagreb, Hrvatska

Tijekom stanične diobe, sestrinske kromatide razdvajaju se formiranjem metafaznog vretena, bipolarne molekularne makrostrukture samosastavljene od mikrotubula i pridruženih proteina. Trenutačno su u modelima metafaznog vretena opisane tri vrste mikrotubula: kinetohorni, interpolarni i astralni. U ovom radu analizirana su antiparalelna nekinetohorna vlakna mikrotubula koja se nalaze odmah ispod sestrinskih kinetohornih parova, a nazvana su premošćujuća vlakna. Primjenom fluorescentne mikroskopije živih stanica, pokazao sam da je ova struktura prisutna u različito obilježenim HeLa i Ptk1 stanicama, i to s različitim brojem mikrotubula u svakoj liniji. Također, analiziran je odgovor vanjskoga kinetohornog vlakna na lasersku ablaciju u staničnoj liniji Ptk1. Uočio sam zajedničku putanju kinetohornih vlakana, kinetohora i premošćujućih vlakana prema van što ukazuje na lateralnu povezanost između kinetohornih i premošćujućih vlakana. Također, pokazao sam da se udaljenost između kinetohora smanjuje nakon ablacije i da razina smanjivanja obrnuto korelira s udaljenošću mjesta ablacije od kinetohore. Dodatno, pokazao sam da se vanjski element vretena izravna nakon ablacije, i to najbrže i najviše u liniji s najdebljim premošćujućim vlaknom, što ukazuje da su ta dva parametra korelirana. Konačno, usporedio sam neke od rezultata s predikcijama teorijskog modela, kako bih pokazao njegovu robusnost koristeći neke eksperimentalne podatke kao ulazne parametre. Dobiveni rezultati govore da su premošćujuća vlakna važna strukturalna komponenta koja ima ulogu u ravnoteži sila kompresije i tenzije u metafaznom vretenu.

(60 stranica, 26 slika, 1 tablica, 80 literarnih navoda, jezik izvornika: engleski)

Rad je pohranjen u Središnjoj Biološkoj knjižnici

Ključne riječi: mitotsko vreteno, metafaza, premošćujući mikrotubuli, stanice Ptk1, stanice HeLa

Voditelj: prof. dr. sc. Iva Tolić

Suvoditelj: izv. prof. dr. sc. Biljana Balen

Ocjenitelji: izv. prof. dr. sc. Biljana Balen

izv. prof. dr. sc. Mirta Tkalec

izv. prof. dr. sc. Renata Matonićkin Kepčija

Rad prihvaćen: 16.6.2015.

BASIC DOCUMENTATION CARD

University of Zagreb
Faculty of Science
Department of Biology

Graduation Thesis

Organisation of microtubules and force-balance in metaphase spindles of HeLa and Ptk1 cells

Kruno Vukušić
Rooseveltova trg 6, 10000, Zagreb, Croatia

During cell division, sister chromatids are segregated by mitotic spindle, a bipolar self-assembly of microtubules and associated proteins. Current models of mitotic spindle recognize three distinct subpopulations of microtubules: kinetochore, interpolar and astral microtubules. The role of antiparallel non-kinetochore microtubule bundles, termed bridging fibers, positioned under sister kinetochores in HeLa and Ptk1 cell lines, was analysed in this study. Using live-fluorescent imaging analysis it was shown that these bundles are present in differently labelled HeLa and Ptk1 cell lines with distinct thicknesses. The response of outermost spindle element to laser ablation in Ptk1 cell line was also analysed. Joint outward movement of bridging and k-fibers was observed suggesting connection into single mechanical unit. Decrease in inter-kinetochore distance was also observed after ablation. That decrease is inversely correlated with distance of the cut from the kinetochore. In addition, spindle element straightening after ablation was observed in all cell lines but with strongest straightening in HeLa cell line with thickest bridging fiber, demonstrating that response to ablation and thickness of bridging fiber are correlated. Finally, some of obtained results were compared with theoretical model of the HeLa metaphase spindle confirming robustness of the model by using some of our experimental data as inputs. In conclusion, obtained results demonstrate that bridging fiber is important structural component of metaphase spindle involved in balancing compressive and tensile forces in spindle.

(60 pages, 26 figures, 1 table, 80 references, original in: English)

Thesis deposited in the Central Biological Library

Key words: mitotic spindle, metaphase, bridging microtubules, Ptk1 cells, HeLa cells

Supervisor: Dr. Iva Tolić, Prof.

Cosupervisor: Dr. Biljana Balen, Assoc. Prof.

Reviewers: Dr. Biljana Balen, Assoc. Prof.

Dr. Mirta Tkalec, Assoc. Prof.

Dr. Renata Matonićkin Kepčija, Assoc. Prof.

Thesis accepted: 16.6.2015.

Table of Contents

1 Introduction	1
1.1. Cell division	1
1.2. Cell cycle.....	2
1.3. Mitosis in general	4
1.4. Microtubule structure, organisation and dynamics	6
1.5. Current models of spindle assembly and movements in prometaphase	9
1.6. Current model of microtubule population within spindle	12
1.7. Molecular forces and force-generators in mitosis	15
1.8. Tensed k-fiber hypothesis and its limitations.....	20
1.9. Aim of this study	20
2 Materials and methods	22
2.1. Cell culture	22
2.2. Sample preparation for microscopy	22
2.3. Imaging.....	22
2.4. Image analysis	23
3 Results	26
3.1. Characterisation of antiparallel fibers spanning region under kinetochores	26
3.2. Force-balance analysis of laser ablation assay videos	33
3.3. Quantitative analysis of spindle shape in response to laser ablation.....	38
4 Discussion	44
4.1. Bridging microtubules in new force map of the spindle	44
4.2. Spindle element is a single mechanical unit under both compression and tension forces	47
4.3. Theoretical model of spindle element and future prospects.....	51
5 Conclusion.....	55
References	56

1 Introduction

1.1. Cell division

Cell division is the process by which a parent cell divides into two daughter cells. This process is the basis of existence and continuity of all life and it can be reasoned that perhaps the most critical part of this process is the ability of cells to accurately duplicate and then faithfully segregate their chromosomes at each cell division. This ensures stability to genomic information that is fundamental to life. For that reason this process has to be very precise because some loss or gain in DNA material can be either lethal to the cell, in which case it is not detected at level of organism, or cause severe complications for the cell. For example, it is estimated that yeast only mis-segregates one of its 16 chromosomes every 100 000 divisions (Bouck et al., 2008). In humans, tightly controlled and timed cell divisions at level of organism are essential for normal differentiation, complex organ development and loss of these normal controls of cell replication is fundamental defect in various types of cancer, infertility disorders and multiple congenital abnormalities (Lodish, 2014).

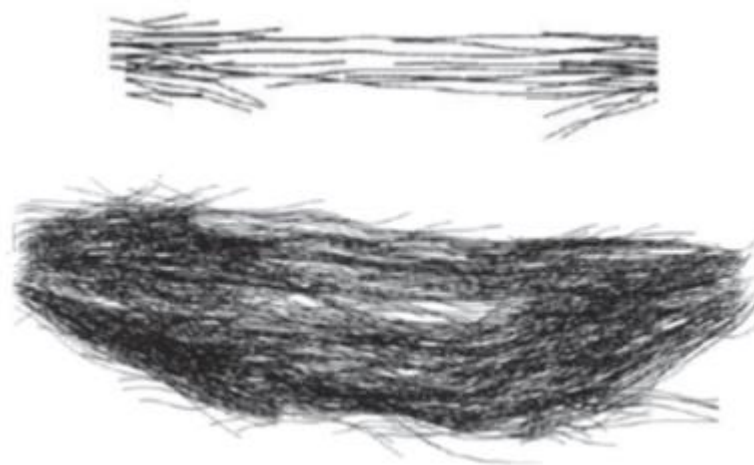


Figure 1. Reconstructions of two mitotic spindles showing different complexity of mitotic spindles in different organisms. *Saccharomyces cerevisiae* (budding yeast, top panel) spindle and *Potorous tridactylus* (PtK2, rat kangaroo kidney, bottom panel) spindle. There are 40 microtubules in the yeast spindle, 32 kinetochore microtubules, and 8 interpolar microtubules versus hundreds in PtK2 (25–30 kinetochore microtubules per chromosome and ~115 interpolar microtubules (ipMTs) from each pole) (Adapted from Bloom et al., 2008).

In all eukaryotic cells, segregation of chromosomes is accomplished by formation of mitotic spindle, highly dynamic bipolar molecular macrostructure of different complexity in

different organisms that is self-organised of microtubules and associated proteins at beginning of mitosis, process that is described below (Figure 1).

Mitosis (Greek *μίτος* mitos meaning thread) is a term first time used by Walther Flemming in 1880 which we now describe as process by which the duplicated chromosomes are segregated to the daughter cells. Even though he worked with cells subjected to rather crude fixation and staining methods, Flemming was able to describe shape of the spindle and its characteristic filamentous organisation (Pawaletz, 2001). In 1950s, polarisation microscopy proved that spindles are built from filaments that run in parallel with chromosome motion and later it was proposed that polymerisation dynamics of these filaments produce mechanical force needed for powering chromosome motions (Inoue and Sato, 1967). Later, by combination of different techniques and rapid expansion in field of molecular biology these filaments were identified as microtubules, non-covalent polymers of protein tubulin (Mohri, 1968). Due to its large size and major role in mitosis, many have studied molecular components of mitotic spindle in last 20 years by various techniques and many proteins were identified that are essential for mitosis (Walczak, 2008). In addition, emergence of techniques such as phase contrast microscopy allowed the first live-cell imaging of a highly dynamic structure such is mitotic spindle. Further, discovery and development of green fluorescent protein (GFP) and its many sister forms allowed for fast visualisation, tracking and quantification of molecular structures within mitotic spindle (Rieder and Khodyakov, 2003). Further, micro-manipulation techniques and laser ablation of some components of spindle gave us insights into mechanical principles of the metaphase spindle, mainly force generation mechanisms involved (Dogsterom and Recouvreur, 2012). However, our understanding of the basic mechanical principles and architecture of this essential cellular structure remains rudimentary, and we cannot explain how the spindle maintains its structural and functional stability in the face of different forces (Shimamoto et al., 2011). By combining all of these techniques coupled with theoretical modelling of the mitotic spindle, modern biophysical research is trying to elucidate some of these questions.

1.2. Cell cycle

Cell cycle is an ordered series of events that lead to cell division and the production of two daughter cells, each containing chromosomes identical to those in the parental cells (Lodish, 2014). The cell cycle is divided into four main phases: G1 (gap one), S (synthesis), G2 (gap

two) and M (mitosis) (Figure 2). To complete the whole cell cycle, HeLa and Ptk1 cells need ~24 hours (Aubin et al., 1980). In G₁ phase (~15 hours) cells grow in size and synthesize proteins and RNAs required for DNA replication. When size of the cell is appropriate and it has synthesized all required molecules, it enters next cell cycle phase by passing a point in G₁ known as START point. When cells pass this point, they are irreversibly committed to cell division. Next, cells enter the S phase (~6 h), where each parental chromosome is duplicated to form two identical sister chromatids duplicated in the process of semiconservative replication. In the next gap phase, G₂ (~2 h), cells synthesize more proteins and grow to prepare for the last phase of cell cycle, M phase (~1 h). M phase consists of two major processes: division of the nucleus, or mitosis, and division of the cytoplasm, or cytokinesis, when the cell itself divides in two. Main function of mitosis is to successfully distribute sister chromatids to each daughter cell (Lodish, 2014). Despite conserved proteins and basic principles of cell cycle and mitosis that are shared by many eukaryotic organisms, the process can differ significantly in some details, so many analogous principles exist that can exert the same function with different mechanisms. Therefore, as this project was done on human HeLa and rat kangaroo Ptk1 cell lines, we will be focusing mainly on mechanisms in those model systems.

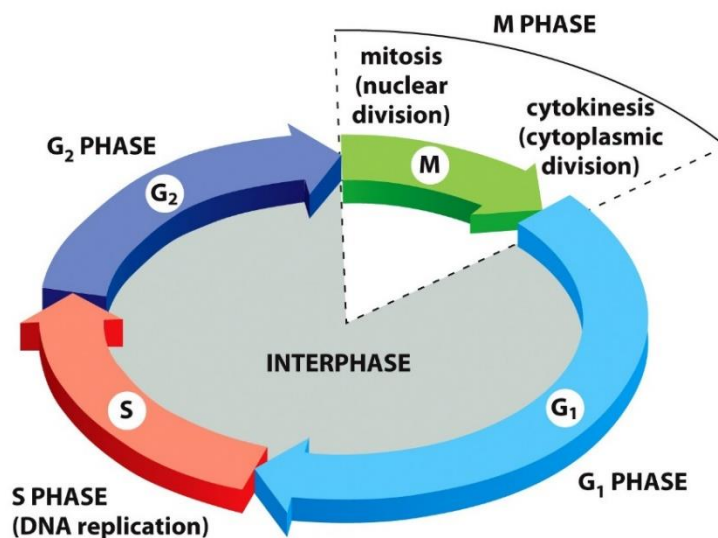


Figure 2. Overview of main phases of the cell cycle in animal cells. S phase of the cell cycle is period of DNA replication followed by gap (G₂) period of protein synthesis. Start of mitosis (in essence nuclear division) is marked with breakdown of nuclear envelope and chromosome condensation and at metaphase-anaphase transition of mitosis sister chromatids segregate. After mitosis, M phase of cell cycle finishes with cytokinesis (cytoplasmic division) followed by gap (G₂) phase of protein synthesis. Interphase is defined as the time between two mitosis (Adapted from Alberts et al., 2010).

It is essential that cell can control each step in cell cycle because it must ensure that DNA replication is carried out correctly and that each daughter cell inherits the correct number

of each chromosome. Accuracy and fidelity are achieved because cell division is controlled by mechanisms known as checkpoint pathways that prevent initiation of next step in cell cycle until earlier step have been completed and errors made during them corrected. The main controllers of cell cycle progression are highly conserved heterodimeric protein serine/threonine kinases that contain a regulatory subunit (cyclin) and a catalytic subunit (cyclin-dependent kinase, CDK). They regulate some key checkpoints, transition from G1 to S phase and from G2 to M phase. This regulative progression, involved in entry of different stages of cell cycle, is achieved by phosphorylating various proteins at specific regulatory sites. Phosphorylation in that way can activate some proteins and inhibit others in complex regulatory networks. Interestingly, CDKs are also subjects of regulation by phosphorylation (Hochegger et al., 2008). In addition, regulated degradation in proteasomes of same proteins plays an important role in cell cycle transitions and because it is irreversible, it ensures that the whole cycle moves in only one direction, from G1 phase to the M phase. Cells produce different type of CDKs that have a role in initiation of specific events in each cell phase (G1 CDKs, G1/S CDKs, S phase CDKs and mitotic CDKs) and CDKs that trigger one cell cycle phase are active only during that phase (Lodish, 2014).

1.3. Mitosis in general

For mitosis to proceed correctly cells must first duplicate their microtubule-organizing red (MTOCs), in animal cells called centrosomes, in coordination with replication of chromosomes in S phase. The duplicated centrosomes separate in prophase of mitosis and will become two spindle poles of mitotic spindle. It is important to note that this process has to be properly regulated because multipolar spindles that result from failure in this process contribute to mis-segregation of chromosomes leading to high genomic instability resulting in aneuploidy seen in many tumour cell lines (Lodish, 2014).

Although mitosis is a continuous process, it has been divided in five stages for ease of description (Figure 3). First phase of mitosis, prophase, is characterized by increased activity of centrosomes, as they begin to nucleate microtubules which replaces interphase array of microtubules with mitotic asters, structures consisting of centrosome and microtubule asters (radial arrays of MTs that converge at the centrosome) (Mogilner and Craig, 2010). Additionally, the dynamics of growing microtubule increase at their plus-end and two mitotic asters are moving to opposite sides of the nucleus by the action of bipolar kinesin-5 motor

protein. Separated centrosomes will form two spindle poles of mitotic spindle. Furthermore, internal order of membrane systems is disrupted; endocytosis and exocytosis stop and actin microfilaments are rearranged to give rise to rounded cell. In addition, chromosomes begin to condense extensively; each DNA duplex must be reduced in length by >1000-fold after which it form tight structures called chromosomes (McIntosh et al., 2012). Next, cohesin complexes at chromosome arms are degraded leaving only those in centromeric region and protein complexes that represent sites of microtubule attachment, called kinetochores, begin to assemble at the centromeric region of each sister chromatid (Dumont and Mitchison, 2009). In prometaphase, nuclear envelope and nuclear pores breakdown and nuclear lamina disassemble. Nuclear envelope breakdown allows microtubules to search and capture the chromosome pairs by associating with their kinetochores (model first proposed in Kirschner and Mitchison, 1986). This first interaction between chromosomes and growing microtubules marks the beginning of assembly of mitotic spindle. When both sister chromatids become captured to opposite spindle poles they are said to be bi-oriented (also called amphitelic attachment) (Mogilner and Craig, 2010). Such pairs begin a process of chromosome congression, movement that finally results in aligned sister chromatids in equatorial plane and finalisation of that process define beginning of the metaphase. Metaphase is defined as a stage when paired sister chromosomes oscillate at the center of the spindle. In this study, I will be concentrating on metaphase because I reason that this is natural starting point to study biophysical properties of the spindle because metaphase is dynamic steady state. That means that despite large fluctuations and directed fluxes in both physical and chemical processes during metaphase average amount and position of spindle components is constant over time (Dumont and Mitchison, 2009). The next stage, anaphase, is induced only when quality control is passed on. That quality control process is called spindle assembly checkpoint (SAC) and it controls segregation in that way that it prevents segregation until chromosomes are attached to poles and kinetochores are under sufficient tension (Cheeseman and Desai, 2009). If these conditions are fulfilled anaphase-promoting complex/cyclosome (APC/C) is activated and cohesin complexes in centromeric part are broken, chromosomes are separated and pulled to different poles by the forces exerted by microtubules shortening in mechanism known as 'pac-man' (anaphase A). Separate movement also occurs: spindle poles move apart from each other through sliding of antiparallel microtubules (anaphase B). In the next phase, telophase, after chromosomes have separated, nuclear envelope reforms and chromosomes decondense. Finally, last phase of the cell cycle, cytokinesis, is characterized by division of the cell cytoplasm through formation of a contractile ring (Lodish, 2014).

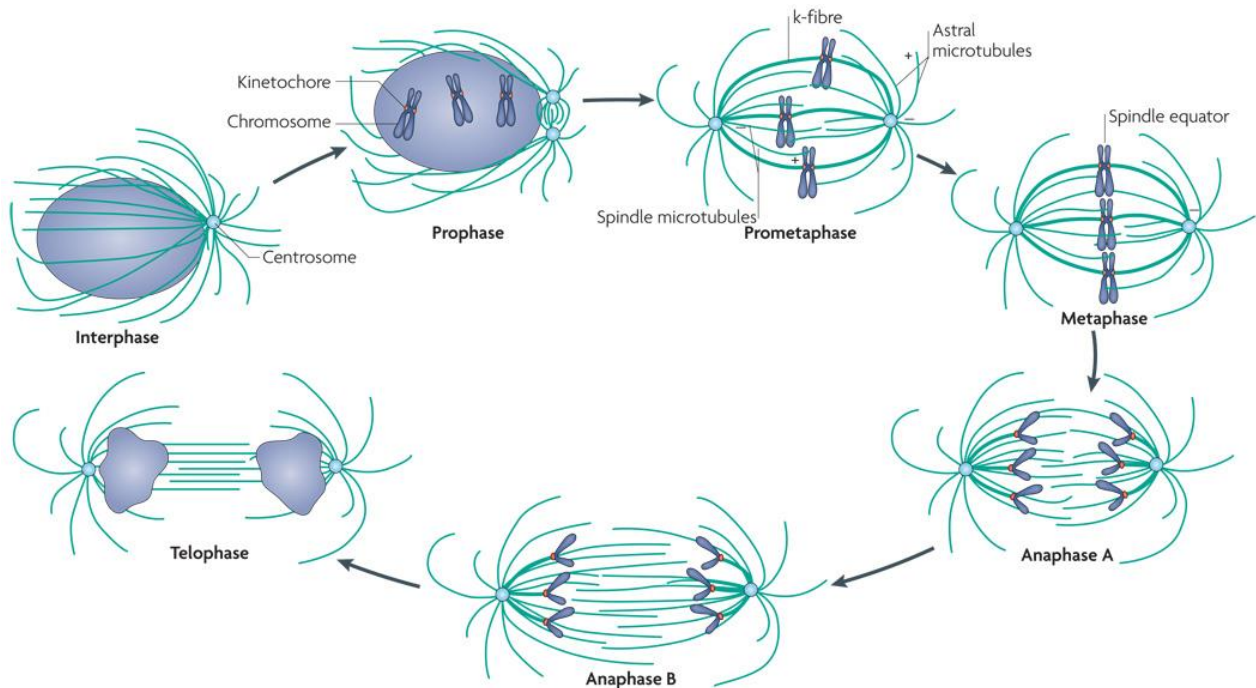


Figure 3. The stages of mitosis with some key components of mitotic spindle noted. Although mitosis is a continuous process it has been divided into stages for ease of description. During interphase, chromosomes are duplicated, binded by cohesin complexes and in the same time, centrosomes are duplicated. During prophase, chromosomes condense as reorganisation of microtubule array occurs. In metaphase, chromosomes are aligned in metaphase plate, and in anaphase, they are segregated to two poles. During telophase contractile ring is formed. More details in the text (Adapted from Walczak et al., 2010).

1.4. Microtubule structure, organisation and dynamics

Microtubules are ubiquitous cytoskeletal polymers essential for the life of all eukaryotic cells. Although they are essential parts of many biological processes and structures, I will focus here on their role in mitotic spindle, as they are fundamental structural and dynamical components of this structure. Every microtubule is dynamic and polar polymer composed of 13 parallel, laterally associated protofilaments that form the hollow cylindrical structure with an outer diameter of 25 nm (Downing and Nogales, 1998). Each protofilament is string of $\alpha\beta$ -tubulin heterodimers connected by non-covalent bonds and arranged in a head-to-tail configuration, with each subunit type repeating every 8 nm. Besides longitudinal head-to-tail interactions between subunits, most microtubules have homotypic lateral interactions between same subunits of different protofilaments (Nogales and Alushin, 2011). As the subunits are oriented in a same way through whole protofilament, they have intrinsic polarity, and as the all protofilaments within microtubule have the same polarity, whole microtubule has an overall

polarity (Lodish, 2014). By convention, the end with exposed β -subunit is called plus-end, while the end with exposed α -subunit is the minus-end. Microtubule polarity is crucial property important for spindle morphogenesis because for example microtubule-based motor proteins, including dynein and a large set of kinesin-like proteins, recognize the surface of microtubules, read their polarity, and move their cargo accordingly (Wittmann, 2001). In addition, because of structural differences between subunits that define two ends of microtubules, growing and shrinking rates are much higher at the plus-end of microtubule. That brings to second important microtubule property important for spindle morphogenesis – dynamic instability. Dynamic instability is a process describing microtubule alternating between slow growing and fast shrinking rates (Mitchison and Kirschner, 1984) (Figure 4).

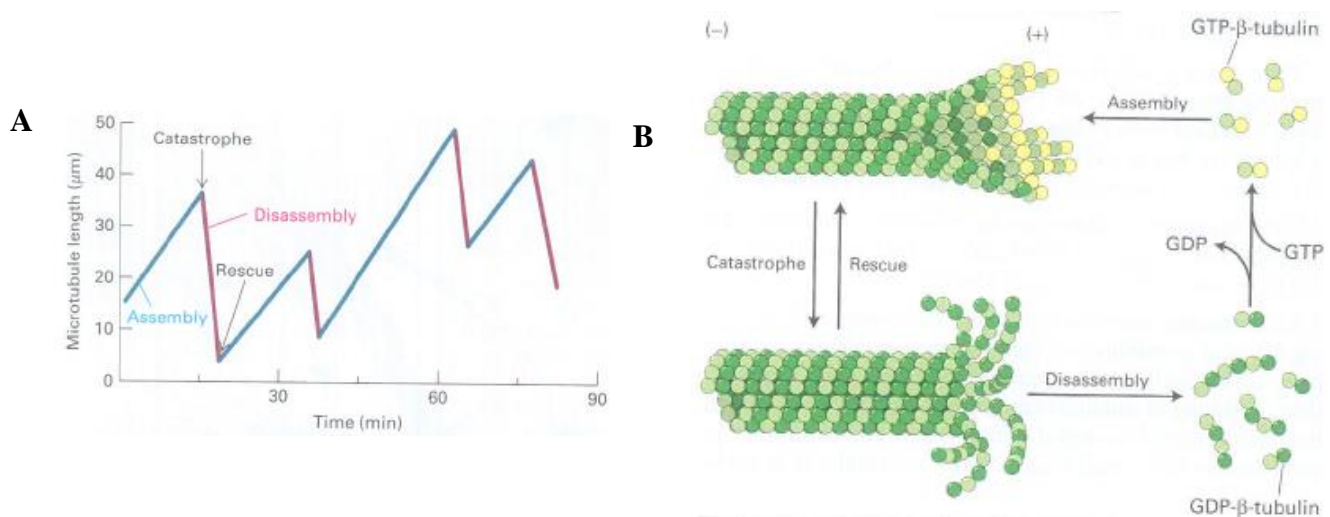


Figure 4. Dynamic instability of microtubules. A) Dynamic instability of microtubules in vitro. Microtubule length is plotted as function of time. Assembly and disassembly each proceed at uniform rates but, as can be seen from different slopes of the lines, shortening of microtubule is much more rapid than growth. B) Growing microtubule with blunter plus-end (top) had GTP- β -tubulin cap whereas shrinking one with curved structure terminate in GDP- β -tubulin. Microtubule dynamics, as can be seen, is higher at the plus-ends of microtubules (Adapted from Lodish, 2014).

To better understand dynamic instability we must first understand the molecular characteristics of tubulin. Each tubulin subunit in the heterodimer can bind one molecule of nucleotide guanine triphosphate (GTP). While in the α -subunit GTP is never hydrolysed because it is trapped by the interface of the subunits, in β -subunit GTP can be hydrolysed and reversibly binded because GTP-binding site is at surface of the dimer. Transition from slow growing to fast shrinking is referred to as *catastrophe*, and transition from fast shrinking to slow growing as *rescue* (Figure 4). Moreover, microtubules sometimes pause for a period of time, during which their length remains constant. Soluble free tubulin subunits have a very slow rate of GTP hydrolysis but this rate increases after subunit becomes incorporated into

protofilament (Deasai and Mitchinson, 1997). Moreover, nucleotide guanine diphosphate (GDP) resulting from hydrolysis of GTP does not exchange while β -tubulin remains in the polymer. So, each protofilament in a growing microtubule has mostly bound GDP β -tubulin subunits while only at the growing tip it is capped by one or two terminal heterodimers containing GTP β -tubulin subunits, this part of growing end is called *GTP cap* (whole model is after it called GTP-CAP model, developed by Mitchison and Kirschner (1984). GTP as such dissociates four times slower than GDP that causes GTP cap at plus-end to stabilize microtubules (Howard and Hyman, 2009). The infrequent loss of such GTP cap would result in a catastrophe, whereas the reacquisition of such a cap by a polymerisation end would result in a rescue. All these processes are carefully regulated by microtubule associated proteins (MAPs) of three class: polymerases that promote growth (CKAP5 for example), depolymerases that promote shrinking (kinesin-13 family for example) and microtubule plus-end tracking proteins that stabilize plus-ends (+TIPs, EB1 for example) (Howard and Hyman, 2009). Importance of dynamic instability can be seen from the fact that energy released by GTP hydrolysis of the subunits behind the GTP cap is stored as structural strain that can be released when cap is lost, process that contributes for example to movements of chromosomes during anaphase.

All microtubules are nucleated from structures known as microtubule-organizing centers (MTOCs) because spontaneous nucleation does not play a significant role in nucleation phase of microtubules assembly *in vivo*. In animal cell, primary MTOC is called the centrosome. In most of the cases, minus-end of microtubule is located near the centrosome and plus-end radiates from it. In interphase, centrosome is located near the nucleus producing interphase radial array of microtubules. Centrosomes are composed of a pair of orthogonally arranged cylindrical structures called centrioles, that are highly stable and surrounded by pericentriolar material (PCM) (Wiese and Zheng, 2006). Despite variations in morphology of centrosomes, all include in their PCM more than 50 copies of the γ -tubulin ring complex (γ TuRC), the conserved, essential core of the microtubule nucleating machinery. Every γ TuRC contains about 13 copies of the γ -isoform of tubulin and several associated proteins. This complex defines the position of MT nucleation, the polar orientation of the polymer, and the fiber into which tubulin assembles (McIntosh, 2012). As I mentioned above, prerequisite for successful mitosis is duplication of centrosomes, in coordination with replication of chromosomes in S phase. These duplicated centrosomes separate in prophase of mitosis and will become two spindle poles of mitotic spindle. Interestingly, it has been noted that at beginning of mitosis microtubule (MT) nucleation rate can increase about 5-fold compared with

that of interphase cells. This can be explained by process called centrosome maturation in which abrupt increase in centrosome-localized γ -tubulin at beginning of mitosis has been noticed (Piehl et al., 2004). In addition, dynamic behaviour of microtubules increases considerably in mitosis, mainly through increasing dynamic instability behaviour. This is accomplished by increased catastrophes (mainly through depolymerisation activity of kinesin-13 family of proteins) and fewer rescues (mainly through activity of stabilizing microtubule-associated protein XMAP215) (Lodish, 2014). Recently, another pathway has been described for nucleation of microtubules including the augmin complex, protein complex consisting of eight polypeptides that can bind to existing microtubules, there it recruits γ TuRC that nucleate assembly of new microtubules. It is one example of centrosome-independent microtubule formation in dividing cells (Hsia et al., 2014). It is believed that this complex is not essential for spindle formation and function but in absence of this pathway, levels of spindle microtubules are reduced (Goshima, 2008).

1.5. Current models of spindle assembly and movements in prometaphase

The mitotic spindle essentially has three principal components: centrosomes, chromosomes and microtubules. As I already described, it forms in prometaphase as chromosomes become connected to two centrosomes by microtubule bundles that link each pole to a specialized macromolecular assembly on the chromosome's centromeric region, termed the kinetochore (Kirschner and Mitchison, 1986). By transmission electron microscopy it was elucidated that kinetochore is trilaminar plate-like structure with electron-opaque outer and inner plates separated by an electron-translucent middle layer with the plus-ends of the kinetochore microtubules terminating in the outer layer (Brinkley, 1966). In human cells, 15–20 microtubules are bound to each kinetochore (Cheeseman and Deasai, 2008), and 24 ± 5 in Ptk1 cells (Rieder, 1981). Initially, using human antibodies researchers have identified three major proteins in the kinetochore, CENP-A, CENP-B and CENP-C. More recent studies have identified more than 80 protein components of the kinetochore complex. In general, connection between microtubules and kinetochores leads to capturing and stabilisation of microtubule that generally results in the formation of the typical spindle in which the poles are focused on the centrosomes on opposite sides of the cell (O'Connell and Khodyakov, 2004). In addition, it seems important to mention the forces that can be exerted on chromosomes by dynamic connection between kinetochores and microtubules. These forces are crucial and not

dispensable for proper chromosome alignment at metaphase plate. One can imagine how this connection complex must be very dynamic, because microtubules in kinetochore fibers (k-fibers) are very dynamic, so to maintain this connection kinetochores must somehow move together with k-fibers when they oscillate, both poleward and inward. That means that when microtubules in k-fiber start depolymerizing, kinetochores that are connected with them must follow this poleward motion in a dynamic fashion because microtubules are shortening, and kinetochores on the other side must coordinate polymerizing motion of k-fiber attached to it. As it can be seen by this description, this complex movements, often called kinetochore oscillations because kinetochores are easiest to track, have to be highly coordinated, and although process is poorly described to date, several members of kinesin family and dynein had been implicated, such as kinesin-13 subfamily members and kinesin-8 subfamily members (see below) (Jaqaman et al., 2010, Cross and McAnish, 2014).

There are few to date described complex mechanisms involved in initial attachment of kinetochore and microtubules (Figure 5). First model of spindle assembly (Kirschner and Mitchison, 1986) predicted that astral microtubules nucleated at centrosomes experience dynamic instability (rapid growing and shrinking) and in doing so they randomly 'search' the space. If they contact kinetochores, either laterally or at their plus-end, they are 'captured', meaning they are stabilized, and rate of catastrophes is reduced. In time, as process is repeated by many microtubules, number of kinetochore microtubules increases while number of astral microtubules decreases (Figure 5). Model in its initial form had some conceptual difficulties. Random search-and-capture model cannot fit in standard duration of prometaphase in human cells (15-20 min) and chromosome characteristic 'mono-orientation' at one pole would never be achieved at prometaphase with this model (O'Connell and Khodyakov, 2004).

Recent studies have described new model involving Ran, small GTPase that enhances the chance that microtubule will encounter the kinetochores. In essence, during mitosis, exchange factor for Ran GTPase is bounded to the chromosomes thereby generating a higher local concentration of Ran-GTP in the vicinity of the chromosomes. As enzyme required for Ran hydrolysis is evenly distributed through cytoplasm as gradient of Ran-GTP is formed and is centered around the chromosomes, primarily centromeres (Figure 5). Ran-GTP in turn can directly promote microtubule nucleation at centromeres or can stabilize microtubules as they would grow more frequently towards the chromosomes and experience catastrophe when growing away from the Ran-GTP cloud (Caudron et al., 2005). CDK11 has been identified as

a Ran-GTP-dependent MT stabilisation factor (Yokoyama et al., 2008). Although, this mechanism is not essential for spindle formation, it is supplementation mechanism that works in cooperation with search-and-capture model to assemble spindle relatively fast. This mechanism dependent on the Ran-GTP gradient is thought to be effective over a long range (~20 μm) but Ran-GTP cannot make a substantial gradient over a shorter range (< 5 μm) presumably because of its rapid diffusion (Tanaka et al., 2010). In addition, microtubule random pivoting mechanism around the spindle pole has been described in yeast cells (Kalinina et al., 2013). By this mechanism, microtubules 'search' the space for kinetochores, and become stabilized when they capture the kinetochore. This mechanism can fit within typical time required for kinetochore capture by microtubule in yeast cells (Pavin and Tolic-Nørrelykke, 2014) (Figure 5). Also, in some model systems (yeast, *Drosophila* and some vertebrate cells) kinetochore-derived microtubules had been reported that subsequently can interact with MTs extending from spindle pole along their length thereby facilitating kinetochore (KT) loading on to fiber of MTs extending from spindle pole (Kitamura et al., 2010) (Figure 5). Problem of opposite polarity (minus-ends at kinetochores and plus-ends extending further) that would result from this nucleation could be conciliated by creation of short MTs (~50-500 nm) that are generated initially with this opposite polarity which is afterward converted, at least in some model systems (*Drosophila* and vertebrate cells). In support of this, γ -tubulin complex is found at KT in vertebrate cells and conversion of polarity is thought to be promoted by some plus-end directed motor acting on KT (e.g. CENP-E).

Once the kinetochore is attached either laterally (more frequently) or terminally (less frequently) by mechanisms mentioned above, the minus-end directed motor protein complex cytoplasmic dynein-dynactin, associates with kinetochore and moves the sister chromatids down the microtubule (poleward KT transport) (Yang et al., 2007). As microtubule plus-end is shrinking, it catches up with the laterally associated KT connected to MT lattice, leading to end-on attachment, the connection where KT is connected with MT plus-end. Soon afterward chromosome is pulled toward a spindle pole as MTs continues to shrink (end-on pulling). This movements help to orient the sister chromatid so that the KT that is not occupied by microtubule is pointing toward the distal spindle pole. These mechanisms are included in pushing chromosome arms by microtubules in orientation process and are thought to highly increase accuracy of spindle assembly (Paul et al., 2009). When a free kinetochore is captured by a microtubule from a distal pole, the sister chromatid pair is said to be bi-oriented (e.g. amphitelic attachment). In addition, when some chromosome achieve amphitelic attachment and is under

tension, other chromosomes in the spindle can use his kMTs to contribute to their proper orientation and movement inside the spindle center. This spindle-equator-directed gliding movement is mediated by kinesin-7 motor protein (also known as CENP-E) that are associated with free kinetochore and move chromosome to the plus-end of the kinetochore microtubule (Cai et al., 2009).

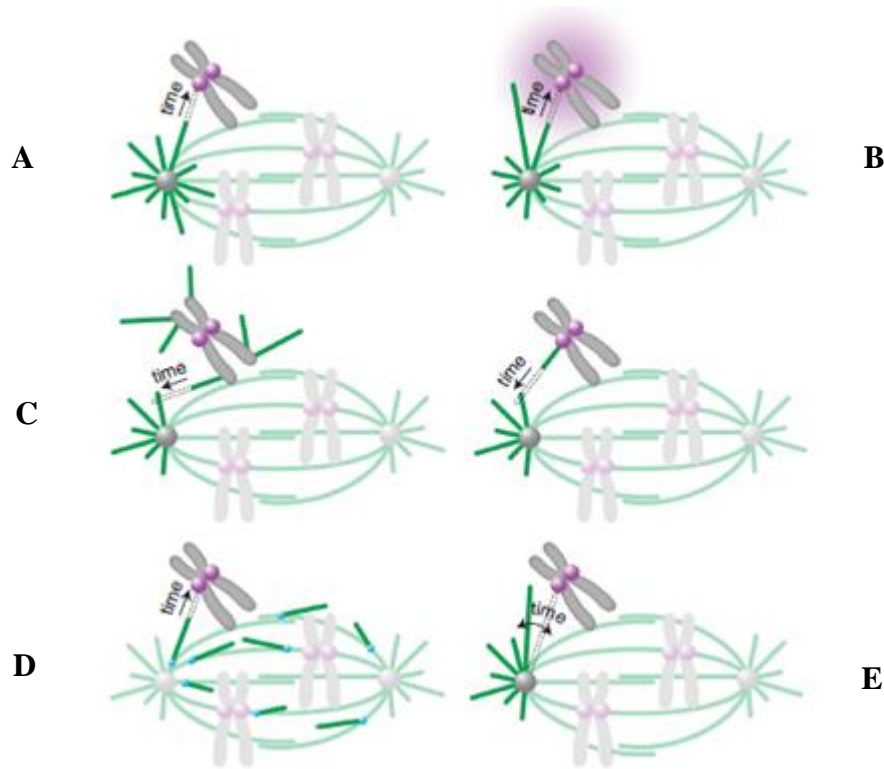


Figure 5. Different models of kinetochore capture by microtubules. A) Search and capture model of kinetochore capturing. B) Biased model of kinetochore capture involving cloud of Ran-GTP in vicinity of kinetochores. C) Microtubule nucleation at chromosomes (left panel) and at kinetochores (right panel). D) Microtubule nucleation at already established kinetochore microtubules. E) Pivoting mechanism of microtubules around the spindle pole. (Adapted from Pavin and Tolic-Nørrelykke, 2014).

1.6. Current model of microtubule population within spindle

Current models of animal spindles describe three distant populations of microtubules within mitotic spindle: kinetochore, nonkinetochore and astral microtubules (Figure 6). Although they all assemble from the same pool of tubulin subunits, they differ in their architecture, dynamics and role they play in mitotic spindle (Mitchison and Dumont, 2009) (Figure 6).

Kinetochore microtubules (kMTs) have their plus-ends embedded in outer kinetochore layer and minus-ends at or near centrosomes. Main function of this population is to exert pulling forces on chromosomes at kinetochore and they seem to be indispensable for proper spindle function. As already described, they do this by forcing chromosomes to congress to metaphase plate and then to pull separated sister chromatids to different poles of the spindle at anaphase. They also silence the spindle assembly checkpoint (SAC), a special signalling system that is active on sister kinetochores without attached microtubules e.g. when kinetochores are not under sufficient tension (Dumont and Mitchison, 2012). Typical number of kMTs that binds to one kinetochore in mammalian cells is from 10-30. KMTs that are connected to the same kinetochore tend to assemble into a bundle called kinetochore fiber (k-fiber) and most of MTs within one fiber are continuous from kinetochore to the pole and run in parallel orientation. Microtubules within fiber are evenly spaced at 50-100 nm apart and interactions between them are weak along k-fiber, except near spindle poles where these interactions are strong (McDonald et al., 1992). Crosslinking proteins that have been shown to lock parallel microtubule together include kinesin-14 family members Ncd and Klp2 (Fink et al., 2009, Braun et al., 2009). If k-fiber is perturbed in some 'natural' or artificial way it behaves as single mechanical unit (Nicolas et al., 1982). Origin of kMT has been described in previous section because origin of kMT reflects origin of spindle itself. These microtubules are not stationary tracks as was once believed yet they have a dynamical property named poleward flux. In poleward flux, polymerisation is happening at plus-end of MT where it is connected to kinetochore and it is balanced in steady state such as metaphase by depolymerisation at minus-end of MT at the poles. Result of this process is constant movement of k-fiber to the pole at about $0.5 \mu\text{m min}^{-1}$ (hence term poleward) (Rogers et al., 2005), which can provide force that can do work when steady state balancing at kMT polymerizing plus-end is suppressed (Waters et al., 1996).

Another microtubule population within spindle are nonkinetochore or interpolar microtubules (ipMTs or just polar microtubules), which comprise a majority of microtubules in large spindles such as vertebrate spindles. They are defined as all microtubules within the body of mitotic spindle that are not kMTs (Dumont and Mitchison, 2012). Electron microscopy studies have revealed that ipMTs tend to bundle together in fibers just like k-fibers do, but each fiber typically contains 2-6 microtubules, evenly spaced by 30-50 nm (Mastonarde et al., 1993) and anti-parallel bundling seems to be predominating, focusing primarily on region of spindle midzone. Their function in spindle is poorly understood and since they are numerous in spindle, it can be reasoned that our knowledge in this area is very limited. It is thought that they primary

function is to keep spindle pole apart through sliding between their antiparallel bundles by action of molecular motors to regulate spindle length and structure and to generate a force that moves poles apart in anaphase B (Dumont and Mitchison, 2009). Their minus-ends are mostly located throughout whole spindle and seldom at spindle poles (Figure 6). In addition, many of these minus-ends are embedded in k-fibers where they are possibly linked mechanically with k-fiber. Like kMTs, they also slide poleward at an average rate of about $2 \mu\text{m min}^{-1}$ but unlike kMTs they do not slide together as a harmonized fiber since velocity of neighbouring ipMTs can vary greatly indicating weakly cross-linking to kMTs and each other (Yang, 2007). It is important to note that most of our understanding of this microtubule population come from study of *Xenopus* egg extracts, where this population of microtubules comprise $> 90\%$ of all microtubules.

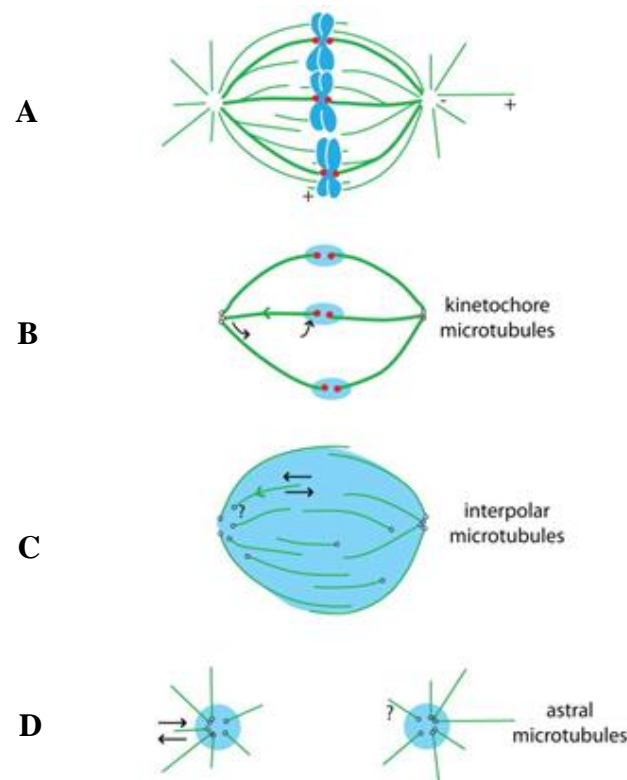


Figure 6. Model of typical architecture of mammalian spindle at metaphase with visual representation of different microtubule populations within spindle. A) Classical model of metaphase spindle with overview of locations of plus- and minus-ends within spindle. Black circles depicts locations of minus-ends of different microtubule populations, blue zones depict nucleation sites and black arrow dynamics of plus-ends. B) Kinetochore microtubules have minus-ends at poles, plus-ends at kinetochore and they continuously slide toward minus-end (poleward flux, depicted by green arrow). They are stabilized by attachment to kinetochore and longer lifetimes than other populations. They usually form large bundles of microtubules called fibers. C) Interpolar microtubules microtubules have very dynamic plus-ends and dynamics of their minus-ends is not extensively studied. They are nucleated through the spindle and continuously slide poleward (green arrow). D) Astral microtubules are nucleated at centrosomes and do not show sliding behaviour (poleward flux). Their plus-ends are dynamic and their minus-ends are fixed at centrosomes. Possible overlapping in definition with other microtubule groups is indicated by question mark (Adapted from Dumont and Mitchison, 2012).

Last population of microtubules described in current models of mitotic spindle are called astral microtubules (aMTs). They are classically defined as microtubules nucleated at centrosomes with their plus-ends extending toward the cell cortex (Dumont and Mitchison, 2012). They turnover by dynamic instability of their plus-ends, at growth and shrinkage rates that are very high, about $10\text{-}15\ \mu\text{m min}^{-1}$ but unlike other populations they do not slide because their minus-ends do not depolymerize. It is thought they perform the critical function of positioning the spindle with respect to the cell division plane by interacting with the cell cortex. There are many models that explain how this is achieved; one of them includes action of cytoplasmic dynein-dynactin complex associated with both cortex and microtubule or some other complexes associated only with microtubules. Dynein then pulls them by walking to their minus-ends embedded in centrosome, thereby pulling whole spindle poleward (Lu and Johnston, 2013). It is important to note that most of our understanding of this microtubule population comes from the study of budding yeast *Saccharomyces cerevisiae* spindle.

1.7. Molecular forces and force-generators in mitosis

Highly purified tubulin heterodimers can assemble *in vitro* into microtubules, but fast assembly and consequent formation of complex structures requires presence of microtubule-associated proteins (MAPs) (Figure 7). Although, MAPs are very broad term that has recently been applied to any protein that can associate, directly or indirectly, to MTs *in vivo* or *in vitro* (Fisher et al., 2008) we can divide them into four groups. The first group consists of crosslinking side-binding proteins that stabilize and align microtubules in specific structures. The second group of plus-end tracking proteins (+TIPs) either regulate microtubule growth at plus-end or links plus-end to the other cellular structures. The third group consists of enzymes that regulate microtubule destabilisation and the fourth of motor proteins that move along microtubules powered by chemical energy (Lodish, 2014). As can be seen from the previous sections where different MAPs were mentioned, they are essential in control of microtubule dynamics and generation of forces that are needed for spindle assembly and proper function of whole spindle.

Force production in mitotic spindle can be divided into active and passive force production. Active force production is defined by processes that convert chemical energy from ATP or GTP hydrolysis into mechanical work (Dumont and Mitchison, 2012). Two main active force production mechanisms are polymerisation dynamics of microtubules (see above in

section 1.4.) and ATPase motor activity. Passive forces are defined by energy consumption that was put into system by one of the active processes. Two main passive spindle forces are elastic contraction and friction and they are often underappreciated in modelling mitotic spindle because they are poorly understood (more about passive forces in Dumont and Mitchison, 2012). It is important to note that all forces that are acting in the metaphase spindle must sum to zero because metaphase spindle is a dynamic steady state, as noted above (see section 1.3.).

Molecular motors are group of proteins that can be broadly described as ATPase enzymes, which bind and catalyse the hydrolysis of ATP into ADP and a free phosphate ion. They couple chemical energy released during ATP hydrolysis to reversible conformational changes in their motor domain(s) to do mechanical work. It is this mechanocemically driven cycling between different conformational states which causes motor proteins to alternate between bound and unbound states allowing them to 'walk' along microtubules. Almost all of them have a motor domain conserved in one family or more motor domains at opposite sides that bind and hydrolyse ATP to walk along more than one track. Besides, they can also have some class-specific nonmotor domains, such as binding domain responsible for binding of their cargo molecules, some domain involved in dimerisation and usually some domain involved in propagation of structural change. Their motion along microtubule is always unidirectional and is connected to intrinsic polarity of microtubules described above. So, some of these proteins are said to walk toward plus- and some toward a minus-end of microtubules. It is this direction of moving that determines the function of each motor protein in spindle assembly and maintenance. Every 'walking' motor has characteristic size of its step, characteristic rate of moving along microtubule and characteristic processivity – can be defined as number of steps motor can do without dissociating from microtubule (Lodish, 2014).

The major plus-end directed motor in the mitotic spindle is the kinesin-5 member Kif11, bipolar homotetramer complex with four heavy chains forming two motor domains that are capable of binding and cross-linking two MTs (Helmke, 2013). It moves along microtubules at rates of 0.1-0.01 $\mu\text{m s}^{-1}$, rates characteristic of mitotic motility and that are almost 10-fold slower than some intracellular transport motors, such is kinesin-1 (Peterman and Scholey, 2009). Kif11, due to orientation of its motor domains, preferentially binds to antiparallel microtubules and then slide them by walking to their plus-ends. Result of such motion is aligning of plus-ends of antiparallel microtubules and pushing apart of their minus-ends (basic anti-parallel sliding filament mechanism). Its main antagonist in sliding antiparallel

microtubules is a motor of opposite directionality such is minus-end directed motor protein kinesin-14 (for example KifC1 in humans). This motor protein slides the minus-ends closer to each other while it pushes the plus-ends apart. This motor functional antagonism is an important mechanism of establishment of initial spindle bipolarity and possibly regulation of spindle length. In addition, it is important to note that activity of these antagonistic motors is changing as mitosis progresses. Following initial dominance of plus-end directed motors, at metaphase steady state is achieved where action of plus-end directed motor proteins is balanced by activity of minus-end directed proteins. In centrosome-controlled spindles such are mammalian spindles, kinesin-5 and kinesin-14 may crosslink and slide anti-parallel ipMTs at the midzone outward and inward, respectively, allowing kinesin-5 to drive poleward flux and pole–pole separation (at least in *Xenopus* and *Drosophila* spindles) and kinesin-14 to shorten the spindle via pole–pole collapse (Peterman and Scholey, 2009). Although, Kif11 is critical to establishment of mitotic spindle bipolarity by centrosome separation it is not required to maintaining of this bipolarity. It has been shown that kinesin-12 plus-end directed protein, Kif15 in humans, plays a major role in maintaining this bipolarity by sliding antiparallel microtubules apart (Drechsler et al., 2014).

Besides already mentioned kinesin-14, the dominant minus-end-directed motor in the mitotic spindle is cytoplasmic dynein. These motors have the same overall organisation, they have two motor domains on one side and nucleotide-insensitive microtubule-binding tail domain on other. As we said before, by binding two antiparallel MTs, minus-end movement of these motors directly functions to oppose the MT motion of kinesin-5s. These proteins have one interesting feature; they can bind one MT as a cargo that is transported toward the minus-end of another MT, thereby clustering the minus-ends of MTs together (sometimes called slide-and-cluster mechanism). These motors therefore have a main role in focusing MTs into a united pole, function obviously very important in maintaining bipolar shape of the spindle (Civelekoglu-Scholey and Scholey, 2010). In addition to this role in organizing MTs in spindle, dynein can also bind different cargoes and transport them to minus-ends of MTs, located mainly at spindle poles. These cargoes can be special protein regulators of spindle assembly and maintenance; such is NuMa, which stabilizes the pole structure, or different motor proteins, mainly kinesins, to transport them back when they came to plus-end of microtubule or to change their activity by changing their location.

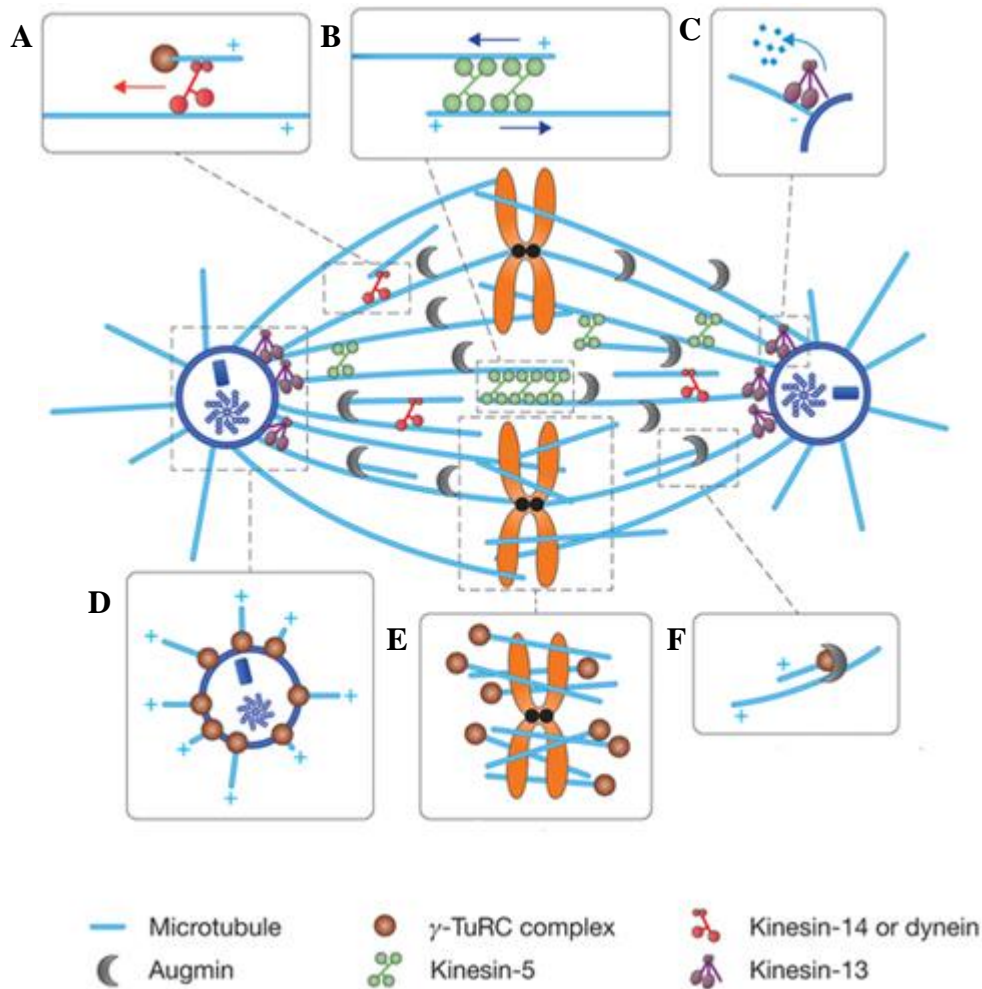


Figure 7. Some of the mechanisms of microtubule-associated proteins (MAPs) in spindle function.

A) Poleward transport of microtubules by minus-end directed motor proteins, for example kinesin-14 or dynein. B) Outward sliding of antiparallel microtubules by action of bipolar plus-end directed kinesin-5 motor protein. C) Depolymerisation at minus-end of microtubule by pole-associated kinesin-13 proteins. D) Nucleation of microtubules at centrosomes mediated by γ TuRC complex. E) Nucleation of microtubules at chromosomes. F) Nucleation of microtubules at sites of existing microtubules, mediated by Augmin complex (Adapted from Wang et al., 2014).

Lastly, a large number of motor proteins has been identified that bind not only to MTs but also to chromosome arms (Helmke et al., 2013). Most important of them are called chromokinesins and are involved in generation of so called polar ejection force (Reider and Salmon, 1994), one of the mechanisms for force production on chromosomes. Chromokinesins are also involved to different degree in some other processes including chromosome segregation, spindle organisation and cytokinesis (Mazumdar and Misteli, 2005). Two members of these groups are plus-end directed Kid/kinesin-10 and kinesin-4 family members, which have conserved motor domains but differ in other domains organisation. Polar ejection force is one of the forces that acts on kinetochores during metaphase (others are poleward flux of k-fiber

microtubules described above and forces exerted through dynamic connection between kinetochores and microtubules described above) to prevent premature movement of chromosomes toward the poles. Kinesin-4 and kinesin-10 bind chromosome arms and interact with microtubules emanating from centrosomes and in doing so they push chromosomes towards a microtubule plus-end and thus toward a metaphase plane (Mazumdar and Misteli, 2005).

Besides motor proteins involved in transportation of microtubules and other cargo in the spindle, there are many classes of MAPs involved in MT destabilisation, MT stabilisation or binding of microtubules to chromosomes.

Proteins involved in MT destabilisation are very important because they disassemble the interphase array of microtubules in prophase and thus providing substrates for formation of all populations of spindle microtubules. In addition, by affecting the lifetime of MTs they can influence the spindle size and organisation in processes such as chromosome attachment, MT flux, MT density and length, behaviour reported after change of their expression in many modelling systems (Helmke et al., 2013). To date, three major classes of this group of proteins have been described: destabilizing kinesin family members (kinesin-13 primarily but also kinesin-14 and kinesin-8), MT-severing enzymes of the AAA ATPase family (Katanin, Spastin, Fidgetin), and tubulin dimer-sequestering proteins (OP18/Stathmin, RB3) (Helmke et al., 2013). Some of these proteins, like kinesin-13 are well known regulators of poleward microtubule flux, mechanism of force release for chromosome positioning (process is described above in section) where they drive depolymerisation at microtubule minus-ends.

In MT-stabilizing group, strictly speaking, we can include nucleation proteins, but these were analysed before, so I will not discuss them. Other MT stabilizing proteins include for example HURP, XMAP215/chTOG, Patronin, and MCRS proteins that are grouped by mechanism that they use to ensure stability of microtubules. First group seems to form protofilament interactions that can stabilize tubulin heterodimers and protofilaments (HURP), second to increase growth rate of primarily ipMTs by interacting with plus-ends (XMAP215/chTOG) and third to reduce catastrophe frequency by interacting with plus- or minus-end (Patronin and MCRS) (Lodish et al., 2014). The two latter groups, because they bind or 'track' plus-ends, are historically known as +TIPS (plus-end tracking proteins). All these stabilizing proteins are required for establishing and maintaining spindle architecture in general.

1.8. Tensed k-fiber hypothesis and its limitations

Knowledge of mesoscopic forces within mitotic spindle is limited compared with knowledge about molecular forces in the spindle. For example, tension pulling forces on metaphase chromosomes were confirmed by experiments using laser ablation where one sister kinetochore was ablated while other moved rapidly toward a pole (Berns, 1981) or by experiments measuring the distance between kinetochores before and after usage of depolymerisation agents whose activity decreased measured distance (Waters et al., 1996). This tension is thought to be generated at interface of kinetochores and plus-ends of microtubules presumably by microtubule depolymerisation (described above in section 1.5.) or action of minus-end directed proteins such as dynein. There is a possibility that depolymerisation or activity of plus-directed motors at minus-ends can generate tension at kinetochores, but this theoretical possibility was never observed experimentally. It is very important to emphasise here, that this tension must be balanced by compression in another part of spindle to maintain steady state. Main candidates for this role are ipMTs because they are often more curved than k-fibers, at least in some systems (Dumont and Mitchison, 2012). This hypothesis of tensed kMTs and compressed ipMTs does not fit all experimental data collected through the years. UV microbeam cutting of some k-fibers resulted in spindle shortening, and same with buckling of remaining k-fibers was observed after rapid depolymerisation of ipMTs using depolymerizing drugs and both are not expected if this model holds in its present form described above (Mitchison, 2005). This led to hypothesis of some non-MT element, termed 'spindle matrix' which that is under tension in spindles and stretches between poles, but such element was has not been observed experimentally to date.

1.9. Aim of this study

Following last section logic we can see that much about organisation of microtubules within spindle and force-balance rules in its different elements is not yet understood on the mesoscopic scale and conflicts in experimental data and theoretical predictions are not so surprising with our currently limited knowledge. In this study, I will be concentrating on metaphase because I reason that this is natural starting point to study biophysical properties of the mitotic spindle because metaphase is dynamic steady state. That means that despite large fluctuations and

directed fluxes in both physical and chemical processes during metaphase average amount and position of spindle components is constant over time (Dumont and Mitchison, 2009). To expand our knowledge about mechanisms and structures that balance forces in the metaphase spindle, especially at region around kinetochores, I decided to clearly define characteristics and force-balance mechanisms within spindle element in different model systems using new approaches. In this work *spindle element* is defined as single mechanical unit comprised of sister k-fibers linked with their kinetochores and connected to a microtubular structure that bridges the gap between kinetochores and interacts with sister k-fibers (first described by the Tolic lab in Kajtez, 2014, Solomatina, 2014). I called that structure *bridging microtubule* (bMT) which, similarly to other microtubule populations, tends to assemble into bundles of microtubules termed bridging fibers. I hypothesized that this structure indeed links sister k-fibers and balances the forces on kinetochores. To confirm that hypothesis I used various approaches. Firstly, I analysed Ptk1 cells on which laser ablation was performed (Rüdiger, 2014) because I wanted to see if new model of bridging microtubules could be applied on Ptk1 cells. Initial observations in works preceding this one in our lab, suggested that it is valid model that can explain antagonistic effects of compression and tension acting on spindle element in HeLa cells transfected with different fluorescently-labelled molecules (Kajtez, 2014, Solomatina, 2014). Also, I want to broaden our knowledge about functional and architectural role of bMT and its characteristics in same HeLa cells so I analysed the videos of same cells where laser ablation was performed but in broader approach and with different strategies. Laser ablation assay (experimental part of this process was not part of this study) is a powerful technique to study metaphase spindle which can be used to disrupt the force-balance in the spindle and in retrospect interpret the forces that were acting on the ablated element by studying its response. I hypothesized that after laser ablation of one side of spindle element the elastic potential energy would be released that was stored in bent k-fibers and stretched centrosomes both in Ptk1 and HeLa cells. As a result of release of that energy, I expect to observe straightening and outward movement of the k-fiber and decrease in distance between sister kinetochores after which I should compare response in different model systems. Finally, my experimental data would be compared with predictions of the theoretical model of metaphase spindle developed together with the Pavin group (Department of Physics, Faculty of Science, University of Zagreb, Zagreb, Croatia).

2 Materials and methods

2.1. Cell culture

I used HeLa-TDS cell line that was previously transfected and stabilized using pEGFP- α -tubulin plasmid which was acquired from Fran Bradke (Max Planck Institute of Neurobiology, Martinsried). Cells were seeded and grown in Dulbecco's Modified Eagle Medium (DMEM) (1 g/l D-glucose, L-glutamine, pyruvate) with 50 μ g/ml geneticin (Life Technologies, Waltham, MA, USA), 100 I.U./ml penicillin (Biochrom AG, Berlin, Germany), 100 μ g/ml streptomycin (Sigma-Aldrich, St. Louis, United States) and 10% Fetal Bovine Serum (FBS) (Life Technologies). The cells were kept at 37 °C and 5% CO₂ in a Memmert humidified incubator (Mettler-Toledo GmbH + Co. KG, Schwabach, Germany).

HeLa cells were transfected by electroporation using Nucleofector® Kit R with the Nucleofector® 2b Device, using the high-viability O-005 program (Lonza, Basel, Switzerland). Transfection protocol provided by the manufacturer was followed except otherwise noted in this text. HeLa cells were transfected with mRFP-CENP-B plasmid (pMX234) provided by Linda Wordeman (University of Washington). 10⁶ cells and 2 μ g of plasmid DNA were used.

2.2. Sample preparation for microscopy

HeLa cells were seeded and cultured in 1.5 ml DMEM medium with supplements (without geneticin, otherwise same as cell culturing medium) at 37 °C and 5% CO₂ on 35 mm glass coverslip dishes coated with poly-d-lysine (MatTek Corporation) for 24-48 hours after DNA transfection. Prior to imaging, medium was replaced with Leibovitz's L-15 CO₂-independent medium supplemented with 10% FBS (Life Technologies).

2.3. Imaging

HeLa cells were imaged by using a Leica TCS SP8 FLIM confocal microscope with a Leica HC PL APO 63x/1.40 CS2 oil immersion objective (Leica, Wetzlar, Germany) heated with an objective heater system (Okolab, Pozzuoli, Italy). During imaging, cells were maintained at 37 °C and 5% CO₂ in H101-1x35-PRIOR-NZ100 digital chamber (Okolab) using H101-BASIC-

BL temperature controller connected with CO2-UNIT-BL controller (Okolab). For excitation, 488 nm line of freely tunable white light laser (WLL) (Leica) and 532 nm of WLL laser (Leica) were used for GFP and RFP, respectively. I used hybrid (HyD) photodetectors (Leica) and rarely photo-multiplier (PMT) detectors (Leica) for detection of fluorescent light. GFP and RFP emission were detected in range of 490-561 nm and 597-695 nm respectively. Xy-pixel size was variable among different images; normally it ranged from 60-100 nm. Pinhole diameter was set to 0.7 μm (1 AU). Pixel dwell time was 1 s. Z stacks were acquired at variable number of focal planes (with intent to encircle whole spindle), always with 0.5 μm spacing. Image acquisition in time, although rarely performed, was done for 20-100 time frames with 10-20 s intervals using unidirectional scanning.

2.4. Image analysis

For image analysis I used videos generated by Jonas Rüdiger on Ptk1 cell line and Janko Kajtez and Anastasija Solomatina on HeLa cell lines (all from Tolic lab at the Max Planck Institute of Molecular Cell Biology and Genetics, Dresden, Germany).

Image processing was performed in ImageJ (National Institute, Bethesda, MD, USA). Quantification and statistical analysis were done in MatLab (MathWorks, Natick, USA) and SciDavis (SourceForge).

Kinetochore position in time and place were tracked using Low Light Tracking Tool, a specialised ImageJ tracking plugin (Krull et al., 2014). Tracking of kinetochores in xy-plane was performed on individual imaging planes for most cells or on maximum projection of up to three plane in rare cases where signal of sister kinetochores was tilted in different imaging planes. Analysis was performed on 50 cells, some cells were rejected because successful ablation could not be observed, kinetochore signal was too weak to track, tubulin signal was too weak to define ablation or spindle was multipolar. Ablation was defined by vanishing of tubulin signal in desired space in channels where it was observed, expansion of ablation hole in all dimensions and movement of kinetochores in response to ablation as described in previous studies (Elting et al., 2014, Sikirzhytski et al., 2014).

The signal intensity of a bridging fiber was measured in ImageJ by drawing a 3-pixel wide line in center of the two outermost sister kinetochore pairs and perpendicular to the line passing through center of kinetochores (visual approximation). Intensity profile was taken along this line and mean value of the background noise signal present near the spindle was subtracted from it. The signal intensity of the bridging fiber was calculated in SciDavis program as the area under the peak which was closest to kinetochores and it was always double-checked to be sure that signal corresponds to the signal of what I saw as a bridging microtubule. The width of this peak at the bottom of the peak was typically 0.6 μm . The signal intensity of the k-fiber was measured in a similar manner, $\sim 1 \mu\text{m}$ away from a one kinetochore pair chosen at random and perpendicular to and crossing the corresponding k-fiber. The width of the peak of the k-fiber at the bottom of the peak was typically 1 μm or more in some cases. In cells expressing PRC1-GFP, mCherry-tubulin and mRFP-CENP-B, measurements were done on four cells where laser cutting was performed and subsequently the k-fibers and the bridging fiber separated, which allowed separation of the kinetochore signal from that of the bridging fiber. The mCherry-tubulin signal of the bridging fiber overlapped with the PRC1-GFP signal, and I defined the width of the former by the width of the latter signal. In addition to these 4 cells, 11 measurements were done on fixed cells in one imaging plane or on a maximum-intensity projection of up to two planes by the procedure described above for other cell lines. Because kinetochores were not labelled in these cells, I measured the bridging fiber intensity in the mCherry channel on the position that corresponds to the midpoint of the same structure in the PRC1-GFP channel. The distance between bridging fiber and center of kinetochores was measured in ImageJ by drawing a 17-pixel wide line (or how much it takes to encompass whole kinetochores) in center of the two outermost sister kinetochore pairs and perpendicular to the line passing through center of kinetochores (visual approximation) in kinetochore channel. Intensity profile was taken along this line with defined length (in most cases 2.5 μm). Then line was kept at exactly the same position with same length but its width was reduced to 3-pixel to encompass only bridging fibers between kinetochores. Intensity profile was taken along this line in tubulin channel and both profiles were processed in SciDavis and ImageJ. I measured the distance between kinetochore peak and bridging fiber peak by extrapolating kinetochore peak position on bridging fiber intensity profile and then measuring the distance between two points lying on parallel line.

The angle between the spindle element and the long axis of the spindle near the centrosome, θ_p , and near the kinetochore, θ_k , was calculated by fitting a line through 3 points

on the measured contour of the spindle element. A typical distance between the neighbouring points on the contours was ~250 nm. Stub length was measured in the first frame after the cut from the center of the corresponding kinetochore to the end of the ablated stub.

Graphs were generated in Matlab (this part was mainly work of Ana Milas, University of Zagreb, Faculty of Science) or SciDavis. ImageJ was used to scale images and adjust brightness and contrast. Figures were assembled in Adobe Illustrator CS5 and Adobe Photoshop CS5 (Adobe Systems, Mountain View, CA, USA). All data are given as mean \pm standard error of the mean (s.e.m.), unless otherwise noted.

3 Results

3.1. Characterisation of antiparallel fibers spanning region under kinetochores

In order to characterize structure of microtubule fibers in mitotic spindle and test hypothesis of bridging microtubule existence in metaphase spindle, I used live-cell confocal laser scanning microscope imaging system and images acquired by special laser cutting assay (detailed description of laser cutting assay in Kajtez, 2014). To test this hypothesis in visual, I turned to two model systems, live HeLa cells stably expressing tubulin-GFP and transiently expressing CENP-B-RFP (a human centromeric protein) and live Ptk1 cells stably expressing Hec1-GFP (a kinetochore protein), which were injected with X-rhodamine-tubulin (Figures 8 and 9). Whole spindle images were acquired but my interest was a region defined by outermost spindle element, especially region around and between outermost kinetochore pair. That region was chosen because that is where bridging fibers could be seen without intrusion from a sister k-fiber signal. As expected, I could observe bMT fiber between and below sister kinetochores in their close proximity on outermost spindle element in both cell lines (Figures 8 and 9). I focused on analysis of the outermost spindle element because spindle elements are very dense in the center of spindle of observed plane and planes below so distinguishing one element from other is imprecise.

The main focus of my analysis was to further describe the characteristics of a bridging microtubule as a microtubular structure in novel model of mitotic spindle initially described in the work of Kajtez (2014) and Solomatina (2014). I turned to analysis of thickness of the bMT fiber in different model cell lines. I used an approach in which I was measuring intensity ratio between k-fiber and bMT fiber because the exact number of microtubules in one fiber due to the limitations of light microscope (resolution ~ 200 nm), could not be determined. Therefore, the obtained result would be an estimation of number of MTs in the bridging fiber. I measured the signal intensity of the MTs between sister kinetochores (I_B), and across the k-fiber in the vicinity (~ 1 μ m from kinetochore (I_{BK})). I interpreted the signal intensity I_B as the signal of the bridging fiber, and I_{BK} as the sum of the k-fiber signal and the bridging fiber signal because I hypothesized that k-fiber and bMT fiber are laterally connected through most of their length, separating at junction point (see later, Figures 10A and 24).

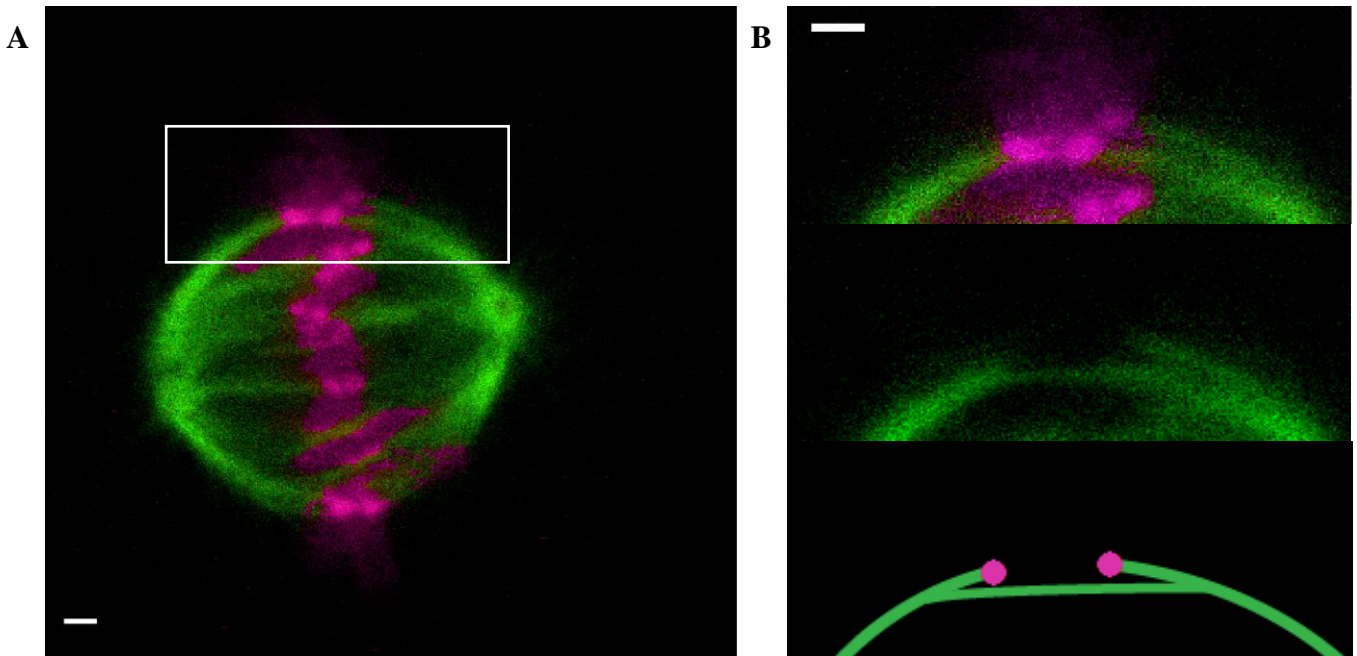


Figure 8. Mitotic spindle of a HeLa cell expressing tubulin-GFP and CENP-B-RFP with a focus on bMT fiber that link k-fibers and kinetochores. A) Image of the whole HeLa metaphase spindle in both channels expressing tubulin-GFP (green) and CENP-B-RFP (magenta). White square indicate region enlarged in B. B) Enlargement of the region at the end of k-fibers with clearly visible bMT between sister kinetochores. Both channels visible (top panel). Enlargement of the region at the end of k-fibers with clearly visible bMT between sister kinetochores. Just tubulin-GFP channel visible (middle panel). Illustration of a model of live picture presented above (bottom panel). Bars indicate 1 μ m.

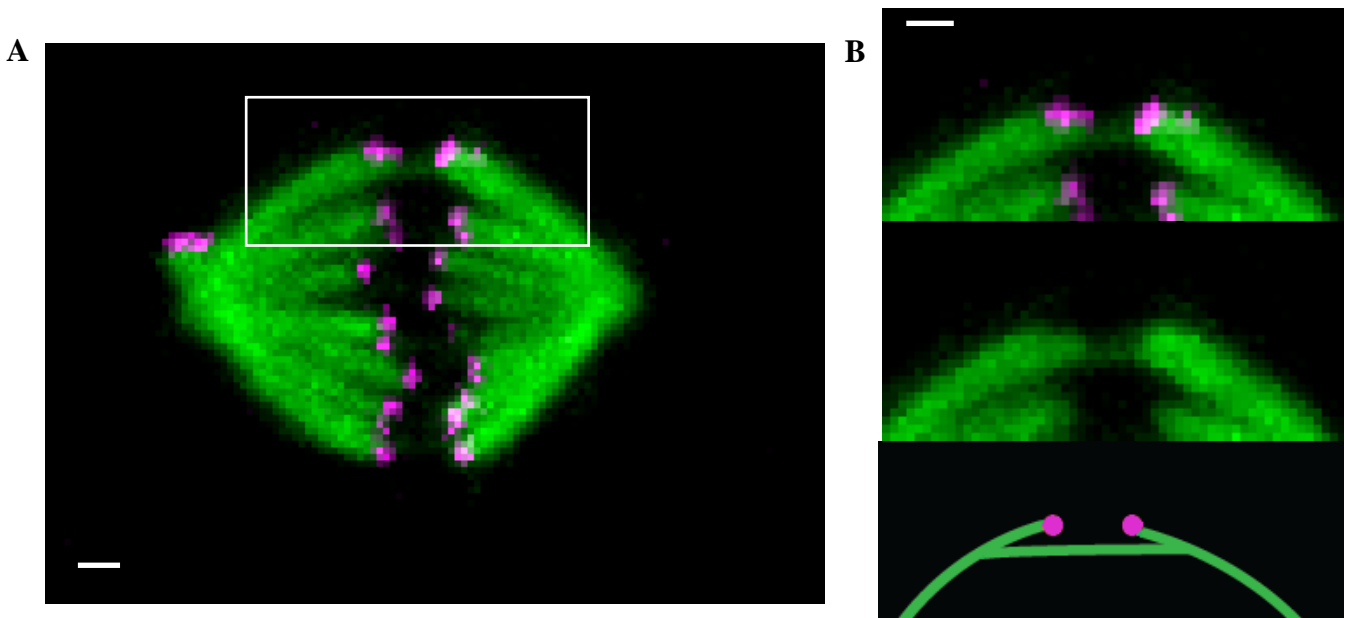


Figure 9. Mitotic spindle of a Ptk1 cells, stably expressing Hec1-GFP, was injected with X-rhodamine-tubulin with a focus on bMT fiber that link k-fibers and kinetochores. A) Image of the whole Ptk1 metaphase spindle in both channels expressing Hec1-GFP (magenta) and injected with X-rhodamine tubulin (green). White square indicate region enlarged in B. B) Enlargement of the region at the end of k-fibers with clearly visible bMT between sister kinetochores. Both channels visible (top panel). Enlargement of the region at the end of k-fibers with clearly visible bMT between sister kinetochores. Just tubulin-GFP channel visible (middle panel). Illustration of a model of live picture presented above (bottom panel). Bars indicate 1 μ m.

First model cell line for these measurements was HeLa cell line stably expressing tubulin-GFP and transiently expressing CENP-B-RFP. Measured in 37 cells, the intensity ratio between bMT fiber and sum of k-fiber and bMT fiber (I_B/I_{BK}) was roughly constant, $I_B/I_{BK} = 45 \pm 2\%$ (Figure 10B). This also shows that in cells where bMT fiber intensity is high, k-fiber intensity is also high, namely there is a correlation between intensity of bridging fiber and k-fiber (Figure 10B). This also indicates that in those cells where the bridging fiber could not be seen, it is because the signal was too weak and not because it was not present there at all. From this ratio, I estimate that the bridging fiber contains $82 \pm 7\%$ (mean \pm s.e.m.) of the number of MTs in the k-fiber (I_B/I_K). Formula for mean is $I_B/I_K = (I_B+I_{BK})/(1-I_B+I_{BK})$. From previous measurements (McEwen et al., 2001), I know that k-fibers in HeLa cells contain 17 ± 2 MTs, so this implies that bridging fiber consist of 14 ± 2 MTs.

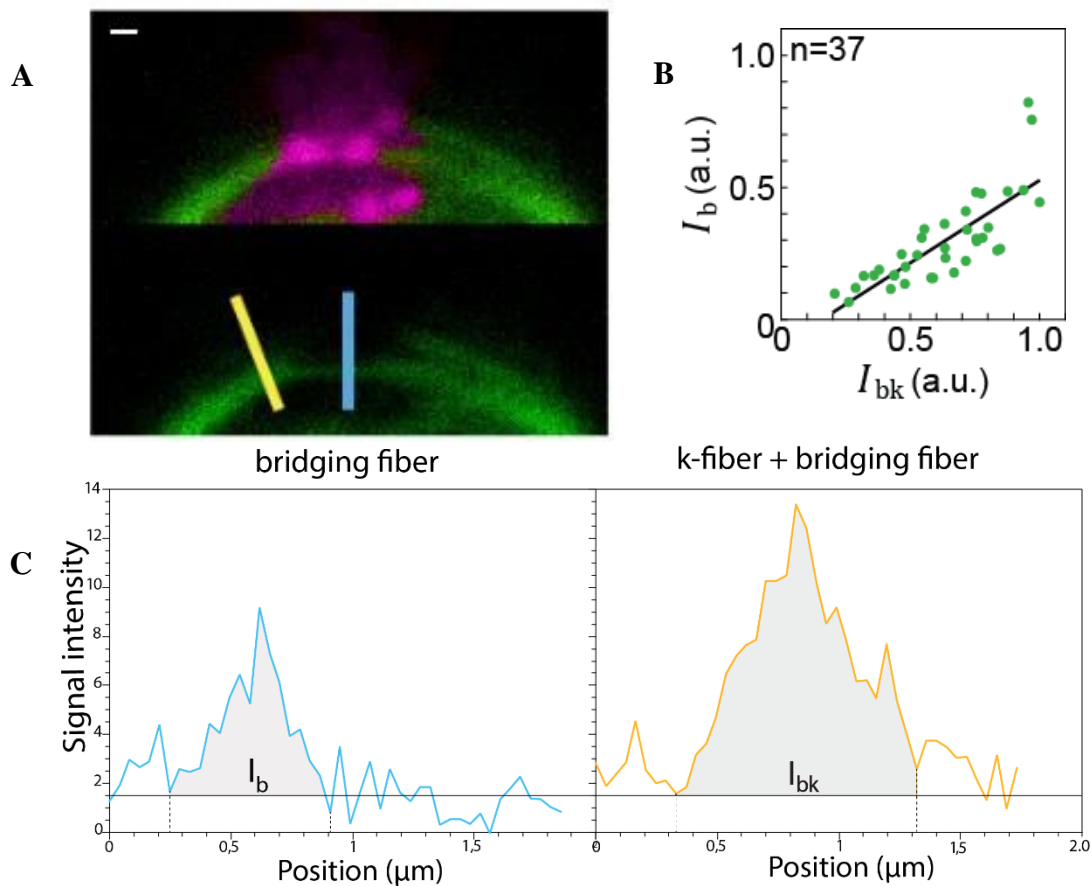


Figure 10. bMT measurement in HeLa cell expressing tubulin-GFP and CENP-B-RFP. A) Picture explaining principle of bMT thickness measurement in corresponding cell. Light cyan line indicates where signal intensity of bridging fiber was measured, I_B , and yellow line indicates where sum of bridging fiber and k-fiber intensities was measured, I_{BK} . B) Signal intensity of the bridging fiber, I_B , as a function of the signal intensity of the bridging fiber and the k-fiber together, I_{BK} , in HeLa cells. C) Measurement of the tubulin-GFP signal intensity of the bridging fiber (left graph, measured along the blue line in the image) and the bundle consisting of the bridging fiber and the k-fiber (right graph, measured along the orange line in the image) in HeLa cell. Horizontal lines mark the background signal; vertical lines delimit the area (grey) where the signal was measured. Bar indicates 1 μm .

Next, I did the same measurements in Ptk1 cells stably expressing Hec1-GFP (a kinetochore protein), which were injected with X-rhodamine-tubulin. Measured in 30 cells, the intensity ratio between bMT fiber and k-fiber (I_B/I_{BK}) was roughly constant, $I_B/I_{BK} = 20 \pm 2\%$ (Figure 11). From previous measurements (McEwen et al., 1997), I know that k-fibers metaphase Ptk1 cells contain 24 ± 5 MTs, so this implies that bridging fiber in these cells consist of 6 ± 1 MTs. This result confirms previous estimates in these cells, where it was observed that 3-8 MTs are laterally associated with kinetochore (Dong et al., 2007). In addition, in these cells I measured the distance between the center of the line joining the two sister kinetochores and the center of the bMT fiber that lies beneath and in between two sister kinetochores using similar intensity approach as in bMT thickness measurements (approach described in detail in Materials and methods). Analysed on 23 cells the distance was $0.20 \pm 0.10 \mu\text{m}$, what is comparable to the same measurements done in HeLa tub-GFP line (0.24 ± 0.15 ($n = 42$), Kajtez, 2014).

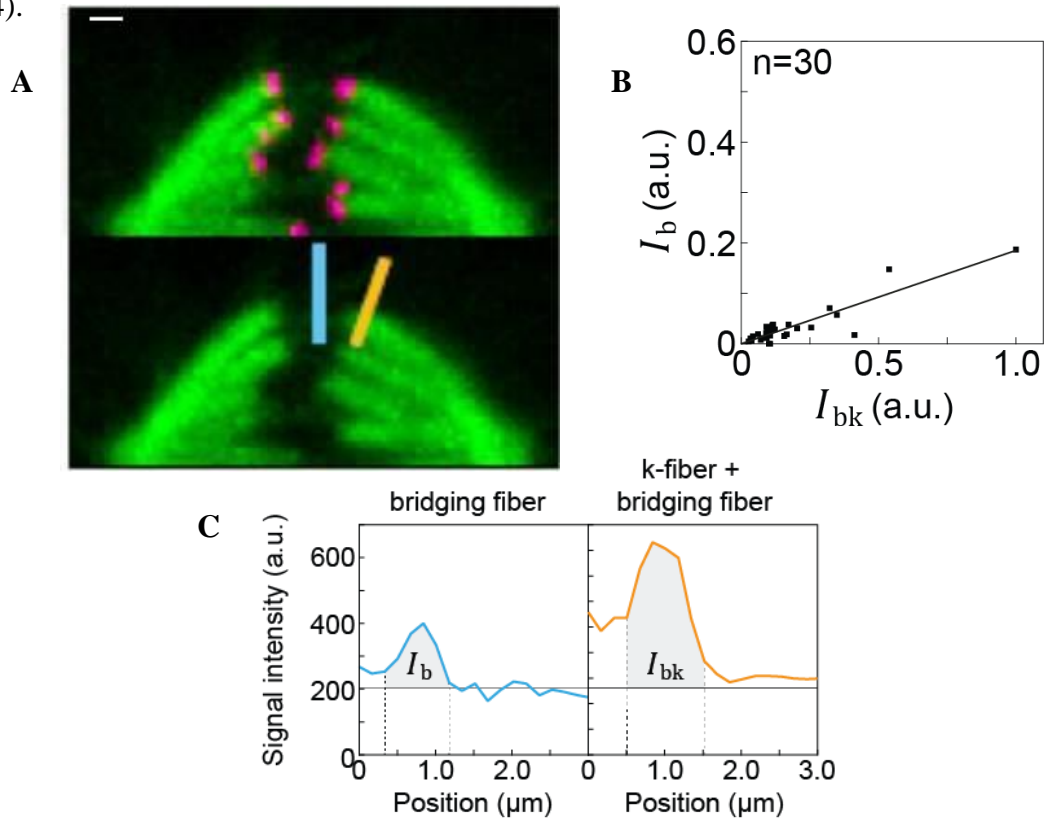


Figure 11. bMT measurement in Ptk1 cell expressing Hec1-GFP, which was injected with X-rhodamine-tubulin. A) Picture explaining principle of bMT thickness measurement in corresponding cell. Light cyan line indicates where signal intensity of bridging fiber was measured, I_B , and yellow line indicates where sum of bridging fiber and k-fiber intensities was measured, I_{BK} . B) Signal intensity of the bridging fiber, I_B , as a function of the signal intensity of the bridging fiber and the k-fiber together, I_{BK} , in a Ptk1 cells. C) Measurement of the tubulin-GFP signal intensity of the bridging fiber (left graph, measured along the blue line in the image) and the bundle consisting of the bridging fiber and the k-fiber (right graph, measured along the orange line in the image) in a Ptk1 cell. Horizontal lines mark the background signal; vertical lines delimit the area (grey) where the signal was measured. Bar indicates $1 \mu\text{m}$.

For confirmation of results and extension of my characterisation of bMT fibers in different conditions I examined thickness of the bMT fiber in the HeLa cell line stably expressing tubulin-GFP and transiently expressing CENP-B-RFP that were in addition treated with proteasome inhibitor MG132 (e.g. synchronisation in metaphase). Measured in 15 cells, the intensity ratio between bMT fiber and k-fiber (I_B/I_{BK}) was roughly constant, $I_B/I_{BK} = 40 \pm 2\%$ (Figure 12), which could be compared with results obtained in untreated cells (Figure 10). This tell us that a bMT fiber is a general structure present in HeLa cell line with a roughly the same thickness. To reduce cell treatment, it was decided that all other analysis on these cells, due to the similar bMT thickness, would be done on untreated cells.

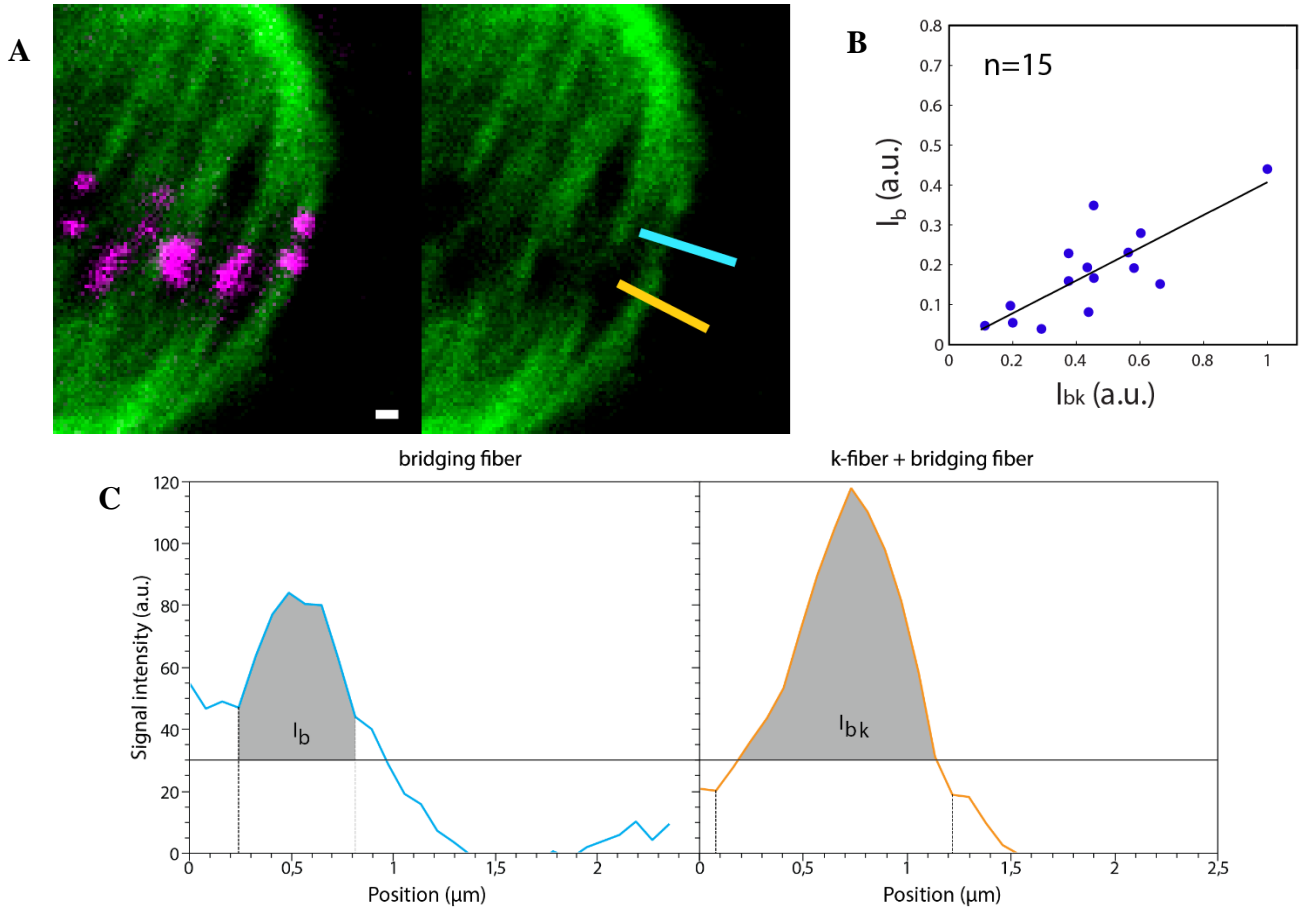


Figure 12. bMT measurement in HeLa cell line stably expressing tubulin-GFP and transiently expressing CENP-B-RFP and that were in addition treated with proteasome inhibitor MG132. A) Picture explaining principle of bMT thickness measurement in corresponding cell. Light cyan line indicates where signal intensity of bridging fiber was measured, I_B , and yellow line indicates where sum of bridging fiber and k-fiber intensities was measured, I_{BK} . B) Signal intensity of the bridging fiber, I_B , as a function of the signal intensity of the bridging fiber and the k-fiber together, I_{BK} , in a HeLa cells. C) Measurement of the mCherry-tubulin signal intensity of the bridging fiber (left graph, measured along the blue line in the image) and the bundle consisting of the bridging fiber and the k-fiber (right graph, measured along the orange line in the image) in a HeLa cell. Horizontal lines mark the background signal; vertical lines delimit the area (grey) where the signal was measured. Bar indicates 1 μm .

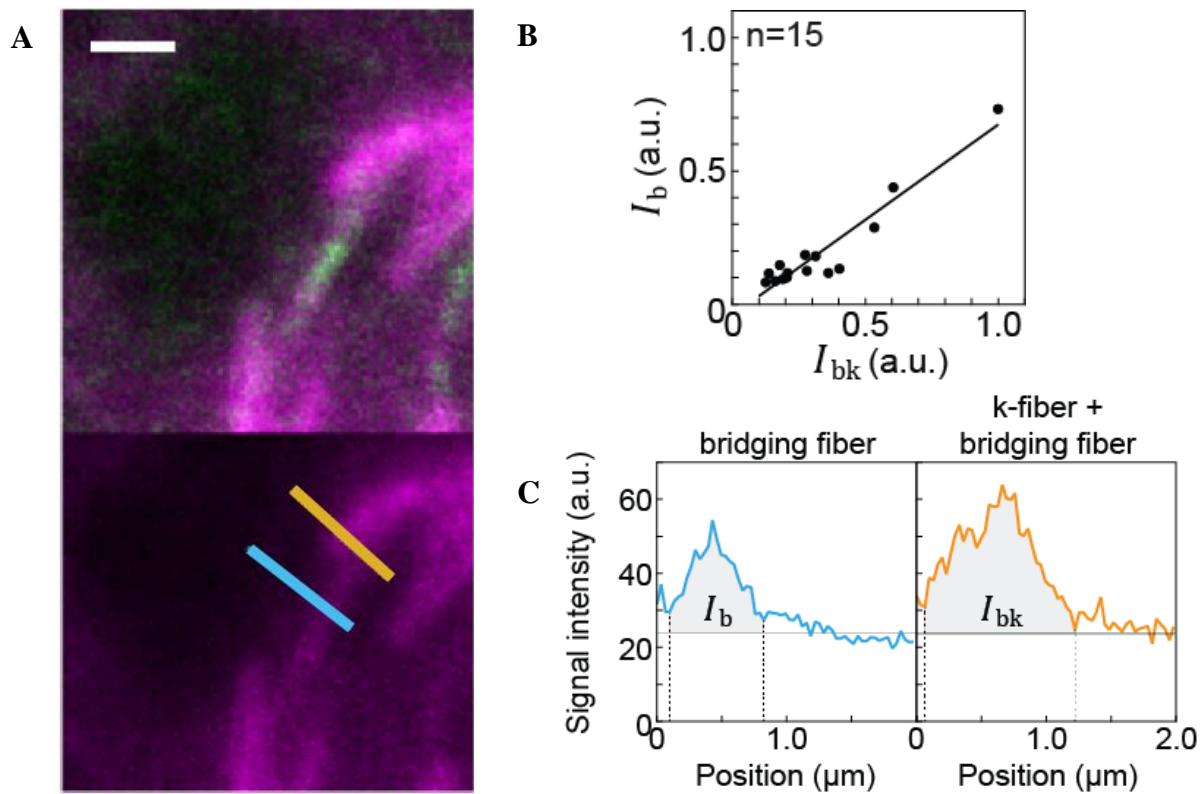


Figure 13. bMT measurement in HeLa cell line stably expressing PRC1-GFP and transiently expressing mRFP-CENP-B and mCherry-tubulin. A) Picture explaining principle of bMT thickness measurement in corresponding cell. Light cyan line indicates where signal intensity of bridging fiber was measured, I_b , and yellow line indicates where sum of bridging fiber and k-fiber intensities was measured, I_{bk} . B) Signal intensity of the bridging fiber, I_b , as a function of the signal intensity of the bridging fiber and the k-fiber together, I_{bk} , in a HeLa cells. C) Measurement of the mCherry-tubulin signal intensity of the bridging fiber (left graph, measured along the blue line in the image) and the bundle consisting of the bridging fiber and the k-fiber (right graph, measured along the orange line in the image) in a HeLa cell. Horizontal lines mark the background signal; vertical lines delimit the area (grey) where the signal was measured. Bar indicates 1 μm .

I also analyzed bMT thickness in HeLa cell line stably expressing PRC1-GFP and transiently expressing mRFP-CENP-B and mCherry-tubulin. I measured bMT thickness in this cell line because I expected to measure thicker bridging fiber in this cell line then HeLa cell line expressing tubulin-GFP and CENP-B-RFP. This can be seen from live-cell fluorescent images taken from these cell lines (Figures 8 and 13A, respectively). I measured bMT thickness both in cells fixed in ice-cold methanol ($n = 11$), and in untreated cells ($n = 4$) (See detailed description in Material and methods). PRC1 is a microtubule crosslinking protein that binds to overlap zones of anti-parallel MTs (Bieling et al., 2010). As I hypothesized before, bMT fiber is made of anti-parallel microtubules, and observed location of PRC1 signal in HeLa mitosis in the center of spindle element between sister kinetochores, confirms my assumption. Measured

in 15 cells, the intensity ratio between bMT fiber and k-fiber (I_B/I_{BK}) was roughly constant, $I_B/I_{BK} = 60 \pm 2\%$ (Figure 13). By the same analogy as before, this implies that there is $n = 23 \pm 5$ MTs in the bridging fiber. Note that in these cells, bMT fiber, as defined previously, is thicker than a k-fiber, which is in agreement with stronger response to laser cutting in these cells, which would be described below.

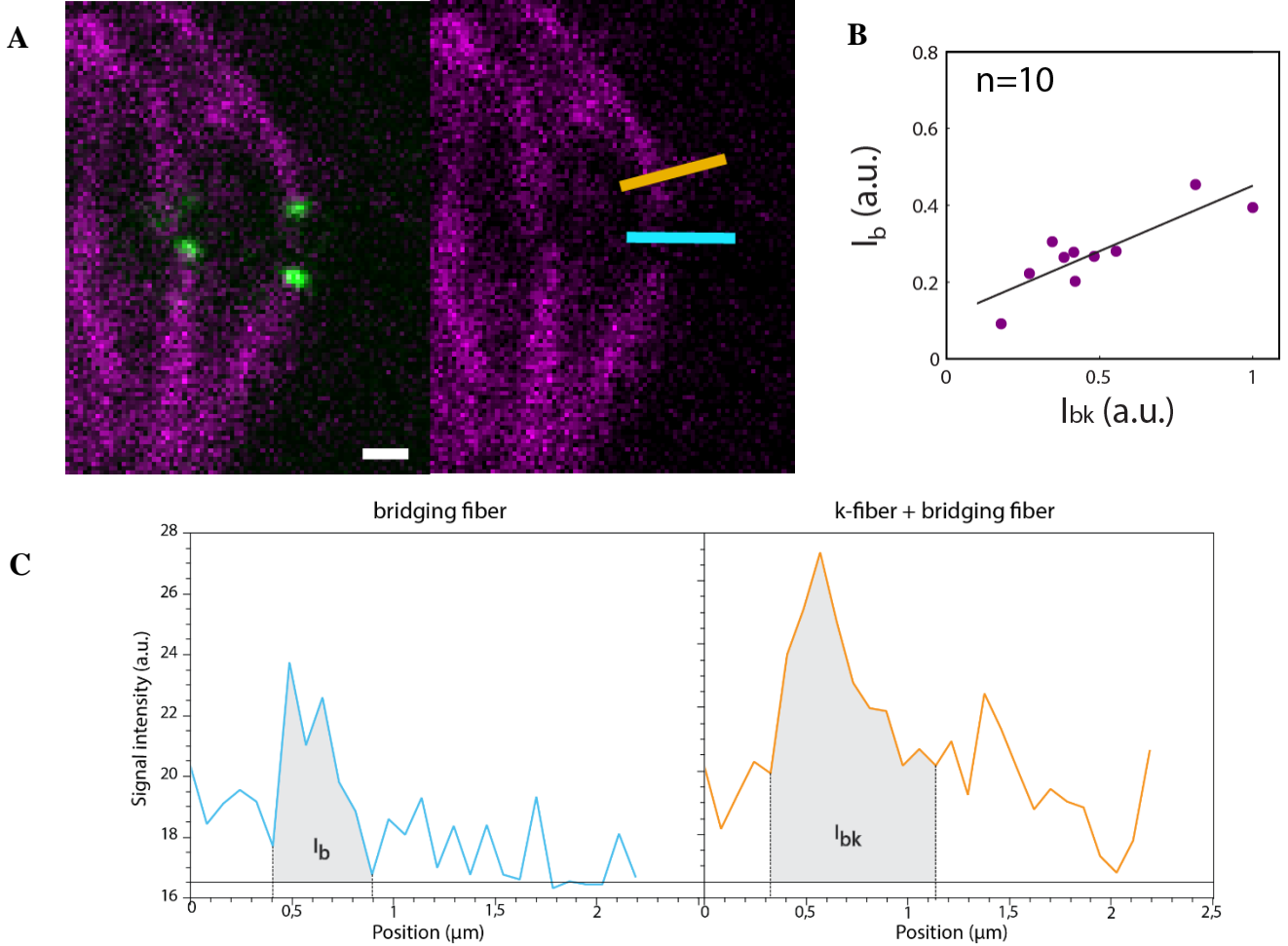


Figure 14. bMT measurement in HeLa cell line transiently expressing CENP-Q-GFP and mCherry-tubulin. A) Picture explaining principle of bMT thickness measurement in corresponding cell. Light cyan line indicates where signal intensity of bridging fiber was measured, I_B , and yellow line indicates where sum of bridging fiber and k-fiber intensities was measured, I_{BK} . B) Signal intensity of the bridging fiber, I_B , as a function of the signal intensity of the bridging fiber and the k-fiber together, I_{BK} , in a HeLa cells. C) Measurement of the mCherry-tubulin signal intensity of the bridging fiber (left graph, measured along the blue line in the image) and the bundle consisting of the bridging fiber and the k-fiber (right graph, measured along the orange line in the image) in a HeLa cell. Horizontal lines mark the background signal; vertical lines delimit the area (grey) where the signal was measured. Bar indicates 1 μm .

To confirm whether thicker bMT fiber is result of PRC1 overexpression or tubulin-mCherry overexpression I analyzed HeLa cell line transiently expressing CENP-Q-GFP (human centromere protein) and mCherry-tubulin. Measured in 10 cells, I found that intensity ratio between bMT fiber and k-fiber (I_B/I_{BK}) was roughly constant, $I_B/I_{BK} = 61 \pm 1.6\%$ (Figure 15) in

these cells. By same analogy as before, this indicates that there is $n = 27 \pm 5$ microtubules in bridging fiber. This is similar to result obtained in HeLa cell line stably expressing PRC1-GFP and transiently expressing mRFP-CENP-B and mCherry-tubulin ($I_B/I_{BK} = 60 \pm 2\%$, Figure 14).

3.2. Force-balance analysis of laser ablation assay videos

So far, I have defined position and thickness of bMT in relation with k-fiber and the whole spindle element. Imaging alone can not provide information about force-balance in the spindle because mitotic spindle is a steady-state system in which there is continuous balance between forces that tend to maintain dynamic steady state. Also, because center of bMT is very close to kinetochores ($0.2 \pm 0.1 \mu\text{m}$, Table 1) and sister k-fiber, it is difficult to observe their relations. To better define role of bMT in force-balance of the Ptk1 metaphase spindle element I used images acquired with laser ablation assay in the Tolic lab (Rüdiger, 2014). The goal of this assay was to selectively perturb the outermost spindle element and isolate it from the rest of the spindle. By doing so, I could interpret the forces acting on spindle element in a retrospect way. For example, movement of sister kinetochores toward each other after the laser cut would indicate the presence of compressive forces acting on k-fiber in region where k-fibers and kinetochores are linked. Ablation was performed at a distance of $2.4 \pm 0.8 \mu\text{m}$ from the nearest attached KT, leaving short k-fiber stub where newly created and relatively stable minus-ends of microtubules are localized (Rüdiger, 2014). By doing so, it would be possible to detach single spindle element from one pole and analyze its response to ablation.

I hypothesized that bMT fibers are laterally connected to sister k-fibers, and that in response to ablation they should move together with kinetochores linked to sister k-fibers, as a single uniform elastic system, called spindle element. Also, I expected that k-fibers are under compression because spindle element is bent in the mitotic spindle, so outward movement of ablated part after releasing the forces that caused bending, should be observed (Figure 15). Also, it was assumed that kinetochores are under tension in metaphase spindle, so decrease in inter-kinetochore distance should be observed shortly after laser ablation. Testing these assumptions would clear the role of compression and tension forces acting on k-fibers and centromeric region of a spindle element and define a role of a bMT fiber in these processes.

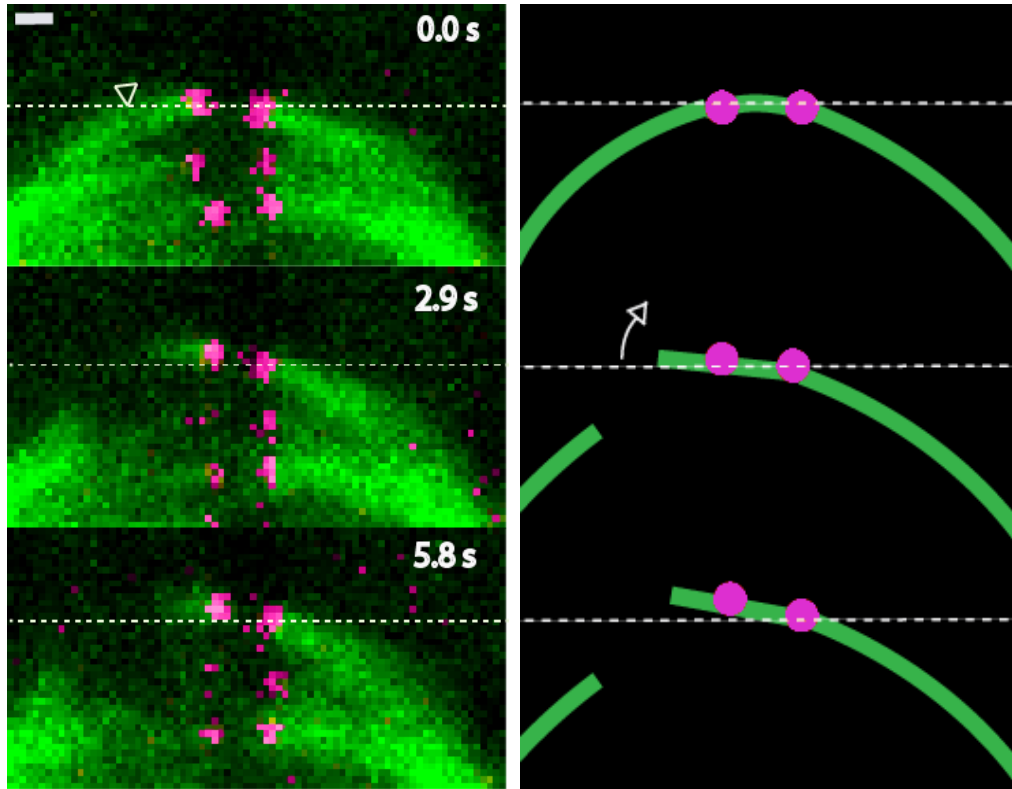


Figure 15. K-fibers, bMT fibers and sister kinetochores act as a single mechanical unit that tends to straighten out and move away from spindle long axis. Time lapse images (left panel) with illustrations depicting model of observed movements (right panel) in Ptk1 metaphase spindle following ablation. Hec1-GFP protein is visible in magenta and injected X-Rhodamine-tubulin in green. Picture depicts coordinated joint movement of k-fiber, kinetochores and bridging fiber away from the spindle long axis. Dotted line represent vertical line connecting center of the sister kinetochores. White triangle represents the site of ablation. White arrow represents direction of spindle element movement after ablation. Note that ablated part of the spindle element is straightening after ablation. Bar indicates 1 μm .

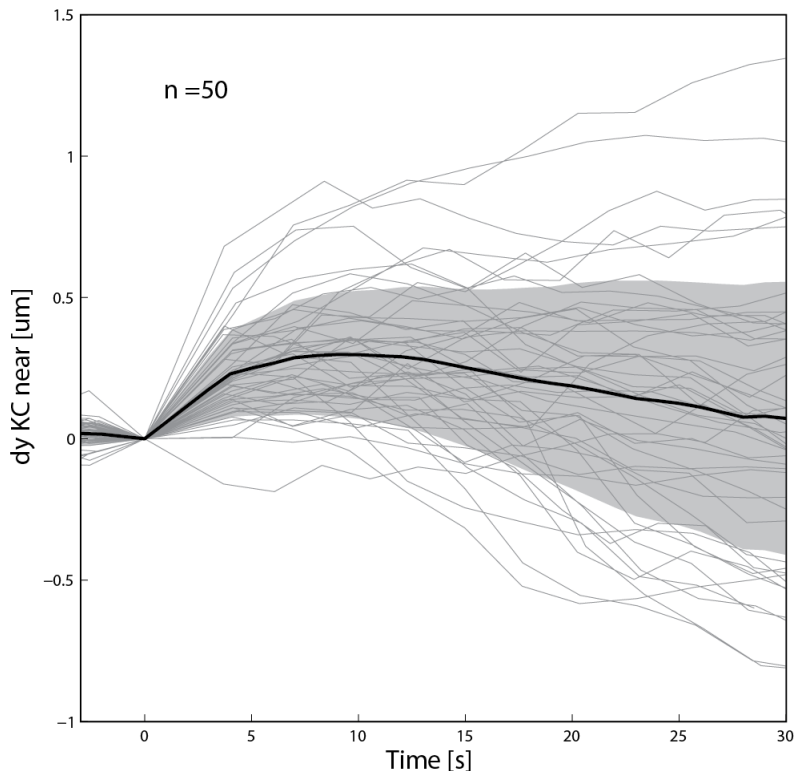


Figure 16. Movement of sister kinetochore pairs from spindle long axis following ablation. Displacement (d) of the kinetochore that was closer to the cut (KC near) site in the direction perpendicular to the long axis of the spindle (y) in Ptk1 cells as a function of time. Displacement is normalized with position of the kinetochore before the cut. Negative value indicates moving toward the long axis of the spindle, and positive values indicate moving away from the long axis of the spindle. Time at the moment 0 indicates moment of ablation. Thin gray lines represent individual cell measurement; black line represents mean value and shaded area represents standard deviation.

To define movement of the spindle element in response to laser ablation, I turned to kinetochore tracking in time. Importantly, I observed that bridging fiber moved outward together with kinetochores, intact k-fiber and k-fiber stub as a single spindle element (Figures 15 and 16). Outward movement was defined as displacement of the kinetochore that was closer to the cut site in the direction perpendicular to the long axis of the spindle (long axis of the spindle is a reference), with respect to its position before the cutting. Outward movement of the outermost spindle element in first frame after the cut was observed in 94% (47/50) of the kinetochore pairs studied, where in rest 6% (3/50) no movement or a minor movement inwards with maximum displacement of 0.1 μm was observed (Figure 16). The maximum displacement was observed in most cases within three frames or ~ 7 s after ablation. After maximum displacement kinetochores slowly started to move back toward the long axis of the spindle (Figure 16).

Next, I hypothesized that sister kinetochores are under tension, and I expected that following spindle element ablation sister kinetochores would move toward each other, in other words, inter-kinetochore distance would decrease after the cut. For this analysis, I used a data acquired from tracking of kinetochore pairs described previously. As I expected, dramatic drop in inter-kinetochore distance was observed following ablation as sister kinetochores move toward each other (Figures 17 and 18). In 92% (46/50) of ablated cells, the distance between sister kinetochores decreased first frame after ablation, and in the 8% (4/50) there were no change in kinetochore distance or kinetochore distance increased after ablation (Figure 18).

Next, I decided to analyze if the degree of sister kinetochore relaxation after ablation, expressed by strenght of tension, correlates with the inter-kinetochore distance before ablation (e.g. streched distance). It could be reasoned that centromeric heterochromatin that lies between kinetochores can be described as ideal elastic spring that would completely return to its relaxed state after ablation, when tension between kinetochores is released. Therefore, it would be expected that degree of relaxation would not depend on streched distance before ablation. However, data clearly indicate correlation between two variables, meaning that kinetochores that were more streched before ablation will remain further from each other after ablation (Figure 19). So, elasticisty of centromeric heterochromatin is not ideal, and I could argue that heterochromatin in this reagon witstands permanent deformations in elasticity induced by high tension forces that pull kinetochores from each other in metaphase.

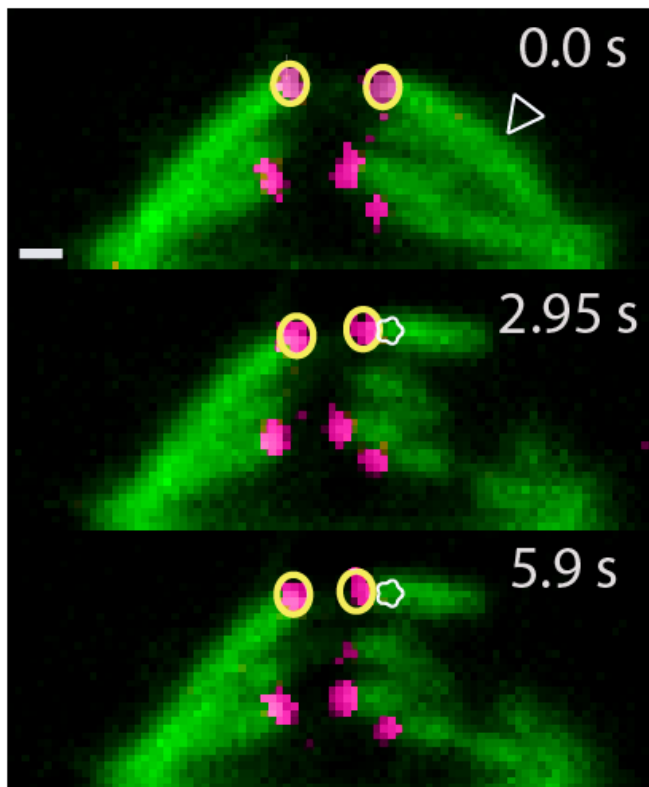


Figure 17. Sister kinetochores tend to get closer after ablation. Time lapse images of Ptk1 metaphase spindle following ablation focusing on kinetochore movements. Hec1-GFP protein is visible in magenta and injected X-Rhodamine-tubulin in green. Picture depicts decrease in inter-kinetochore distance after ablation. White triangle represent site of ablation. White stars represents position of kinetochore near ablation site before ablation. Note that ablated part of the spindle element is straightening after ablation. Bar indicate 1 μm .

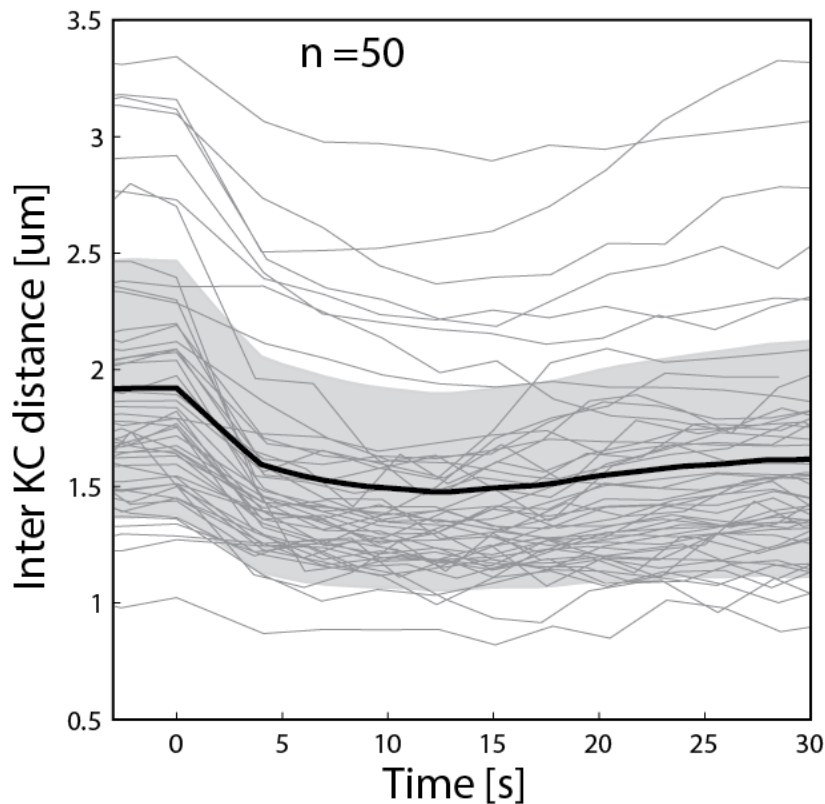


Figure 18. Shortening of inter-kinetochore distance after ablation. Inter-kinetochore distance as a function of time normalized to the value at the moment of ablation (time 0 represent ablation) in Ptk1 cells stably expressing Hec1-GFP, which were injected with X-rhodamine-tubulin. Gray lines represent individual cell measurements, upper and bottom black lines represent borders of standard deviation, and middle black line represent mean value. Note the drop in inter-kinetochore distance in most of the cells.

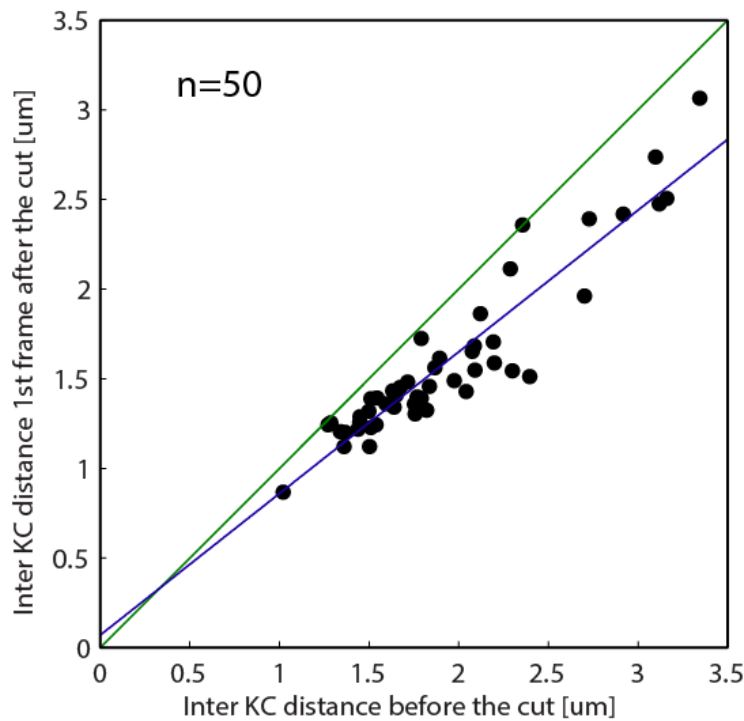


Figure 19. Plasticity of centromeric heterochromatin. Inter-kinetochore distance 3 frames (~ 7 s) after ablation as a function of same distance before ablation for each analyzed cell. Green line represent $x = y$ curve, all points lying below that line represent inter-kinetochore distances that are relaxed post-ablation. Blue line represent linear fit of the data.

Lastly, I analyzed if the position of the cut, measured by ablated stub length, have impact on degree of relaxation of sister kinetochores after laser ablation experiments. In model of metaphase spindle that include bMTs, bridging fibers are laterally connected along length of sister k-fiber, but near the kinetochores two structures separate and the point of separation is named junction point. I can theorise that two distinct possibilities of spindle element response after ablation exist, one in which cut is made before junction point, and one in which cut is made after junction point. In first one, the connection between k-fiber and bMT remain intact and compression of bMT fiber that is bend between two junction points balance the tensions between sister kinetochores. In the second one, the connection is broken and tension force is released. So, I would expect that in the first case degree of relaxation would be small to none, and in the second case degree of relaxation would be much bigger (Figure 20B). As junction point is single point along spindle element, I would observe sharp transition between cells where ablation site is passed junction point from those where it did not. The region of sharp transition would give as estimation of junction point position along spindle element. As I expected, the degree of sister kinetochore relaxation was larger for ablation sites near the kinetochores and smaller for ablation sites further from kinetochore in Ptk1 cells indicating correlation between two variables ($n = 33$) (Figure 20A). Also, as expected, I observed a point

on x-axis that indicates somewhat sharp transition between cells of high and low degree of relaxation. Our analysis have show that cells with ablation sites up to $\sim 1.25 \mu\text{m}$ from the kinetochore 11/22 cells (50%) had more then 35% reduction in inter-kinetochore distance after ablation with a maximum of 90%. On the other hand, cells with ablation sites higher then $\sim 1.25 \mu\text{m}$ had 1/12 (8.3%) had reduction in inter-kinetochore distance greater then 35%.

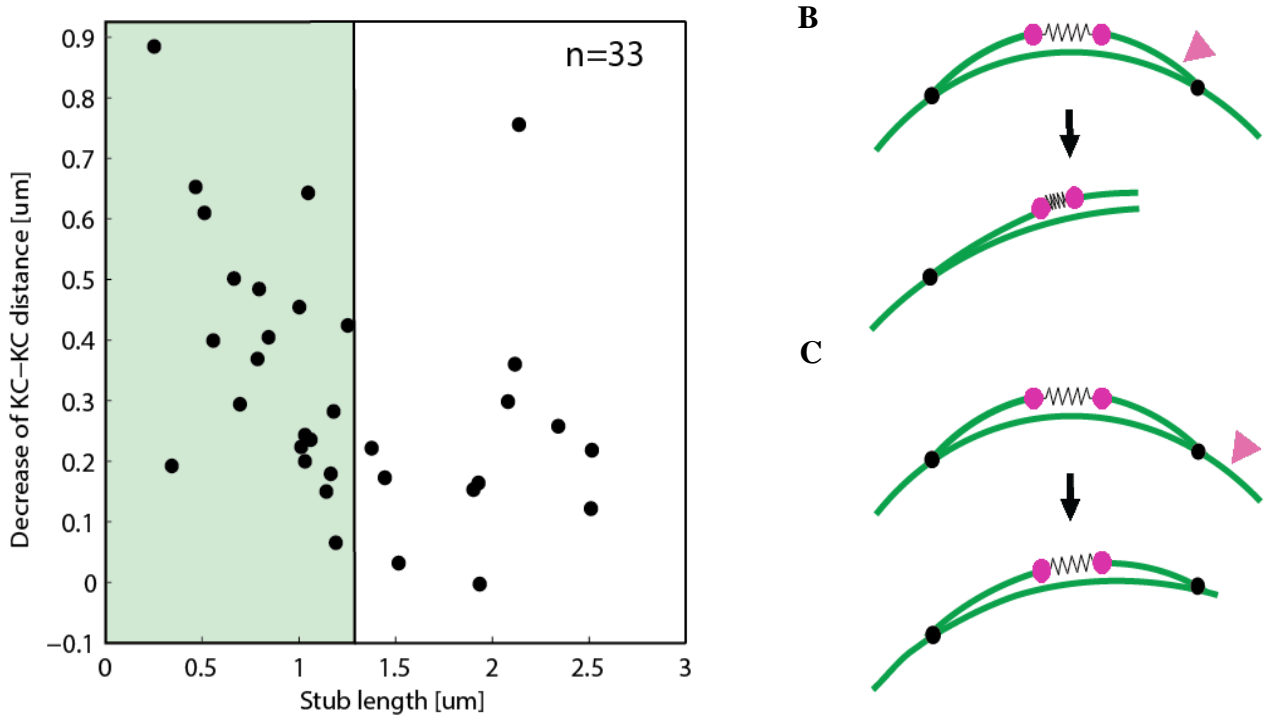


Figure 20. Relation between ablation site position and response of kinetochores to ablation. A) Decrease in inter-kinetochore distance (KC-KC) as a function of a ablated stub lenght in Ptk1 metaphase cells. Decrease in inter-kinetochore distance is defined as ratio of inter-kinetochore distance after ablation versus inter-kinetochore distance before ablation. B) Two hypothetical models depicting response of spindle element to ablation in relation to ablation site with junction point of kinetochore microtubules and bridging microtubules. Cutting between kinetochore and junction point separates k-fiber and bMT fiber which allows release of tensile forces on the kinetochore and inter-kinetochore distance decrease is much higher then in C) where this connection between bMT fiber and k fiber is preserved because ablation site was between junction point and spindle pole. Magenta triangle represents site of ablation.

3.3. Quantitative analysis of spindle shape in response to laser ablation

To quantitatively describe the different shapes of metaphase spindles in HeLa and Ptk1 cells and response of the spindle element shape to ablation I used highly dense tracking along k-fibers in one frame before, and three consecutive frames after ablation. To analyse spindle length and spindle half width I tracked center of the centrosomes and used data from

kinetochore tracking to determine the center between kinetochores. From this analysis I extracted parameters I was interested in: the angle between the spindle element and the long axis of the spindle near the spindle pole, θ_0 , and near the kinetochore, θ_k , the distance between the bridging fiber and the kinetochore, d_{bk} , the distance between sister kinetochores, d_k , as well as the spindle length, L , and spindle half-width, h (Figure 21B). From this analysis I found that shapes of HeLa and Ptk1 metaphase spindles differ (Figure 21A; Table 1) as is expected from taken images (Figures 8 and 9) and confirmed that approach is robust enough to distinguish between delicate changes in shapes of the spindle elements.

I also noticed that in some cells there is an obvious straightening of the spindle element after ablation as I could see clear tendency of ablated stub to line up with intact k-fiber in some cells. That characteristic movement can be seen in the first phase response after ablation in Ptk1 cells, defined by outward movement of the ablated spindle element (Figures 15 and 17). I hypothesized that this movement is not result of presence and characteristics of centromeric heterochromatic spring between kinetochores but rather presence of bMT fiber that is bend between two junction points in spindle element after ablation. Such microtubular structure will tend to straighten out after ablation because it is laterally associated with intact k-fiber on one end, and with k-fiber stub on another. Its presence in spindle element could explain observed joint movements of intact and ablated k-fiber and their kinetochores, as they constitute one uniform elastic system, named spindle element. To quantitatively describe straightening in different cell lines I used data acquired by highly dense tracking of spindle element in time (For detailed description see Materials and Methods). Analysis of this data had shown that the angle at the centrosome did not change significantly in both cell lines after ablation, while the angle at the kinetochore increased by 3.4 ± 1.2 degrees first frame after ablation (~ 4 seconds) and 7.3 ± 2.91 degrees third frame after ablation (~ 8 seconds) ($n = 23$ cells) in original HeLa tub-GFP cells (Figure 21C). In Ptk1 cell line, I observed some perplexing behaviour where the angle at the kinetochores decreased 1.8 ± 2.68 degrees in first frame after ablation and then increased to 4.3 ± 2.42 degrees in third frame after ablation (Figure 21D). Stability of the angle at the centrosome in both cell lines suggests that the spindle element is clamped near the centrosome (e.g. free rotational movements are not permitted).

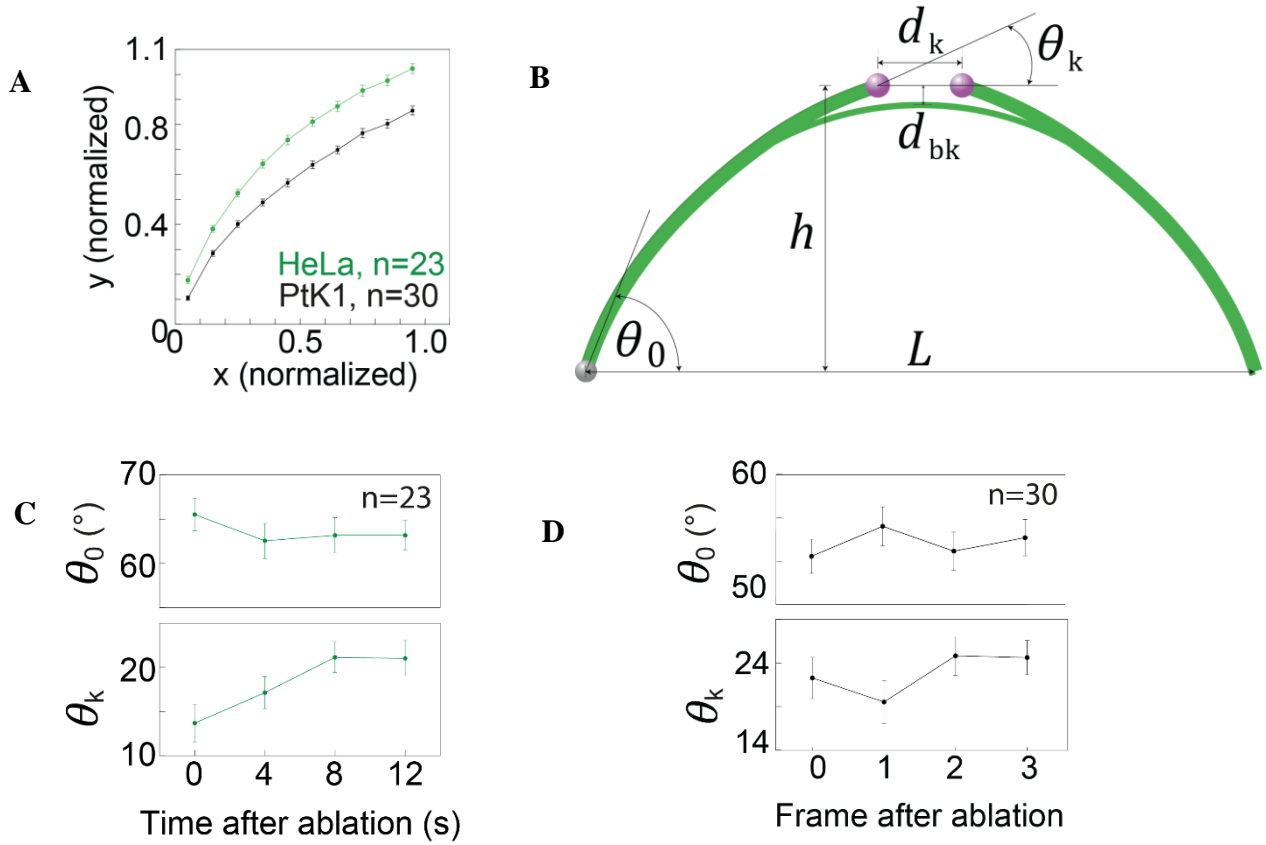


Figure 21. Spindle geometry analysis in different HeLa and PtK1 cells PtK1 cell expressing Hec1-GFP, which were injected with X-rhodamine-tubulin. A) Normalized shapes (mean \pm stdev) of a k-fiber in HeLa (green) and PtK1 (black) cells. The spindle pole is at $x = 0$ and the kinetochore at $x = 1$. Calculated by Ana Milas. B) Scheme of the measured geometric parameters of the spindle, which are listed in Table 1. C) The angles θ_p and θ_k in HeLa tub-GFP cells as a function of time after laser ablation. D) The angles θ_p and θ_k in PtK1 cells as a function of time after laser ablation.

Table 1. Measured geometric parameters in HeLa tub-GFP, HeLa tub-mCherry and PtK1 cell lines. All values are given as mean \pm std, in bracket are number of measured cells for each analysed parameter.

Parameter	HeLa tub-GFP cells	PtK1 cells	PRC1 tub-mCherry
angle between the k-fiber and the long axis of the spindle in the vicinity of the spindle pole, θ_p ($^\circ$)	65.5 ± 8.8 (n = 23)	52.6 ± 8.4 (n = 30)	61.9 ± 6.3 (n = 17)
angle between the k-fiber and the long axis of the spindle in the vicinity of the kinetochore, θ_p ($^\circ$)	13.7 ± 10.1 (n = 23)	21.2 ± 10.2 (n = 30)	13.3 ± 9.8 (n = 17)
spindle length, L (μm)	11.1 ± 1.2 (n = 52)	11.8 ± 1.7 (n = 50)	11.4 ± 0.7 (n = 31)
spindle half-width, h (μm)	5.0 ± 0.7 (n = 52)	4.0 ± 0.6 (n = 50)	4.8 ± 0.7 (n = 31)
distance between the kinetochore and the bridging fiber, d_{bk} (μm)	0.24 ± 0.15 (n = 42)	0.20 ± 0.10 (n = 23)	0.36 ± 0.12 (n = 15)
distance between sister kinetochores, d_k (μm)	1.05 ± 0.32 (n = 52)	1.92 ± 0.54 (n = 50)	0.954 ± 0.236 (n = 31)

Next, I hypothesized that the force in the bridging fiber correlates with the number of MTs in the fiber, so I compared the response to laser cutting in cells with different numbers of MTs in the bridging fiber (see section 3.1. for analysis of bMT thickness). I reasoned that a larger force in the bridging fiber could be observed experimentally as faster straightening of the

spindle element, after the force is released, following laser ablation. I reasoned that elastic microtubule rod such as bMT stores elastic potential energy when it is bent between two fixed points (junction points in this model), and that stored potential energy is greater when microtubule is thicker because stiffer rods have higher tendency to resist mechanical deformations. That larger elastic potential energy stored in the stiffer rods would cause faster straightening of the bMT fiber after ablation when energy is released and consequently, because of interrelation with sister k-fibers and kinetochores, of the whole spindle element. If this is true, I can reason that a bMT fiber is an important linking mechanical element in a metaphase spindle that balances the forces acting on different segments of spindle element. To quantify how fast the spindle element straightens after the cut, I measured the angle defined by the spindle pole and sister kinetochores (angle pole-KC-KC, Figure 22, right panel). The measurement system is designed so that when the spindle element is straight, the sister kinetochores and the spindle pole lie on the same line and the measured angle is 180 degrees, thus larger increase in the angle means faster straightening of the spindle element. I found that in HeLa tub-GFP cell line, which has $n = 14 \pm 2$ MTs in the bridging fiber (Table 1), the angle pole-KC-KC increased by 2.7 ± 0.8 degrees 4 seconds after the cut, i.e., the spindle element became straighter (Figure 22). In Ptk1 cell line, which has $n = 6 \pm 1$ MTs in the bridging fiber (Table 1), angle pole-KC-KC increased by 3.1 ± 2.2 degrees three seconds after the cut (Figure 22). However, variation in bMT thickness that are observed in these cell lines are not high enough to clearly verify this hypothesis, and it can be hypothesized that these measurements cannot distinguish such fine movements at this bMT thicknesses, or such observed movements are countered by those cells where there is no significant movement, at least not as I defined it here.

Because of limited ability of previous approach, I turned to different approach. I analysed videos of PRC1-GFP-tub-mCherry cell line that has a very thick bMT fiber (Figure 13) that is created by simultaneous overexpression of tubulin and PRC1 (Figure 23). Overexpression was done by transiently expressing tubulin-mCherry and mRFP-CENP-B in HeLa cells that stably expressing PRC1-GFP protein (Solomatina, 2014). First, the angle at the centrosome did not change significantly in this cell line after ablation, similar with our previous observation in HeLa tub-GFP and Ptk1 cell lines, while the angle at the kinetochore increased by 11.2 ± 1.1 degrees 3 seconds after ablation ($n = 17$ cells) in this cell line (Figure 24A). In addition, in this cell line, which had $n = 23 \pm 5$ MTs in the bridging fiber (Table 1), the angle pole-KC-KC increased by 14.4 ± 2.1 degrees first frame (4 seconds) after the cut (Figure 22).

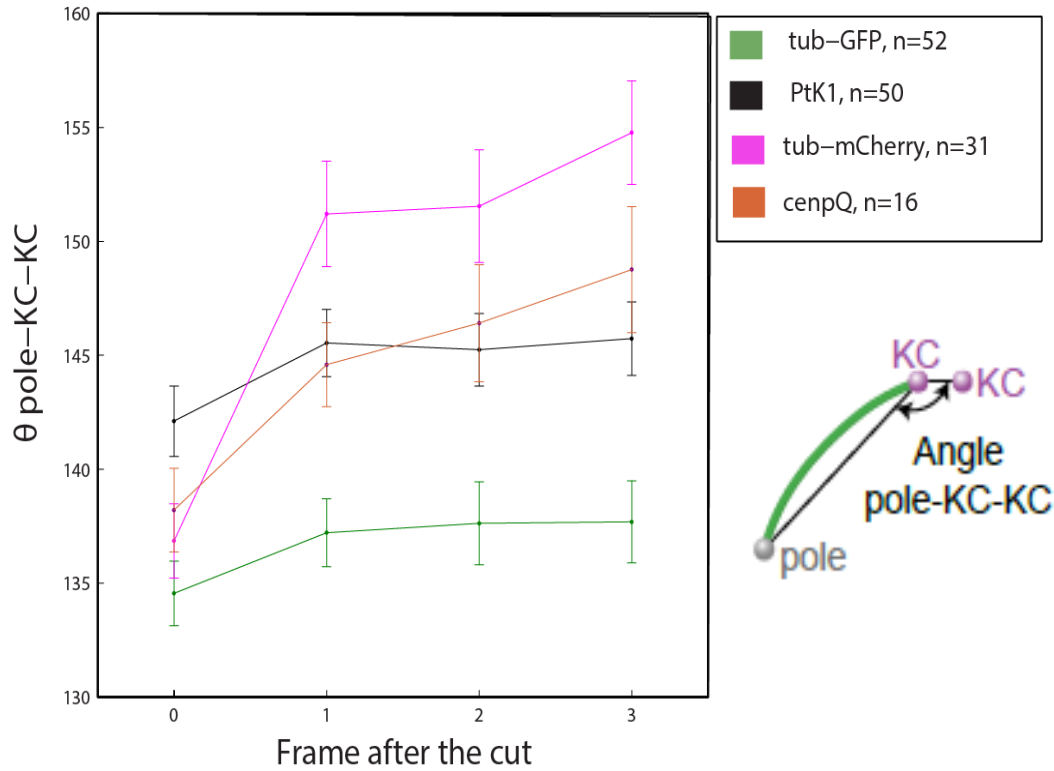


Figure 22. Quantification of spindle element straightening in all HeLa and Ptk1 cell line analysed. Angle θ pole-KC-KC as a function of a frame after ablation. The angle is defined as angle between line connecting pole further from the cut and kinetochore further from the cut with line connecting two sister kinetochores. The scheme on the right is showing how θ pole-KC-KC was defined. Angle θ pole-KC-KC of four cell lines are presented in the graph: HeLa cells expressing PRC1-GFP, mRFP-CENP-B and tubulin-mCherry (magenta), HeLa cells expressing tubulin-GFP and CENP-B-RFP (green), Ptk1 expressing Hec1-GFP which were injected with X-rhodamine-tubulin (black) and HeLa cell line transiently expressing CENP-Q-GFP and mCherry-tubulin (orange).

To compare results with PRC1-tub-mCherry and HeLa tub-GFP cell lines, I also performed the same measurements in HeLa cell line transiently expressing CENP-Q-GFP and mCherry-tubulin. Both cell lines share the same tubulin-mCherry overexpression and I have shown previously that they have thicker bridging fibers than HeLa cell line expressing tubulin-GFP and CENP-B-RFP (Figures 10, 13 and 14). I have found that angle at the centrosome did not change significantly, similarly with all other cell lines studied, while the angle at the kinetochores increased 3.9 ± 3.5 degrees in first frame after ablation and 8.8 ± 4 degrees in third frame after ablation (Figure 24B). This result is similar to those obtained in HeLa-tub-GFP cell line and does not correlate thicker bridging fiber with response to ablation. In addition, the angle pole-KC-KC increased by 6.4 ± 2.6 degrees first frame (4 seconds) after the cut in this cell line (Figure 22). This result is intermediate between results obtained in HeLa-tub-GFP and PRC1-GFP-mCherry-tubulin spindles (Figure 22), and is not expected because this cell line has

bridging fiber thickness very similar to PRC1-GFP-mCherry-tubulin cell line. In PRC1-GFP-tub-mCherry cell line, both measured degrees, that explain the level of response of a spindle element to ablation, are much higher than in HeLa tub-GFP cell line (Figure 22).

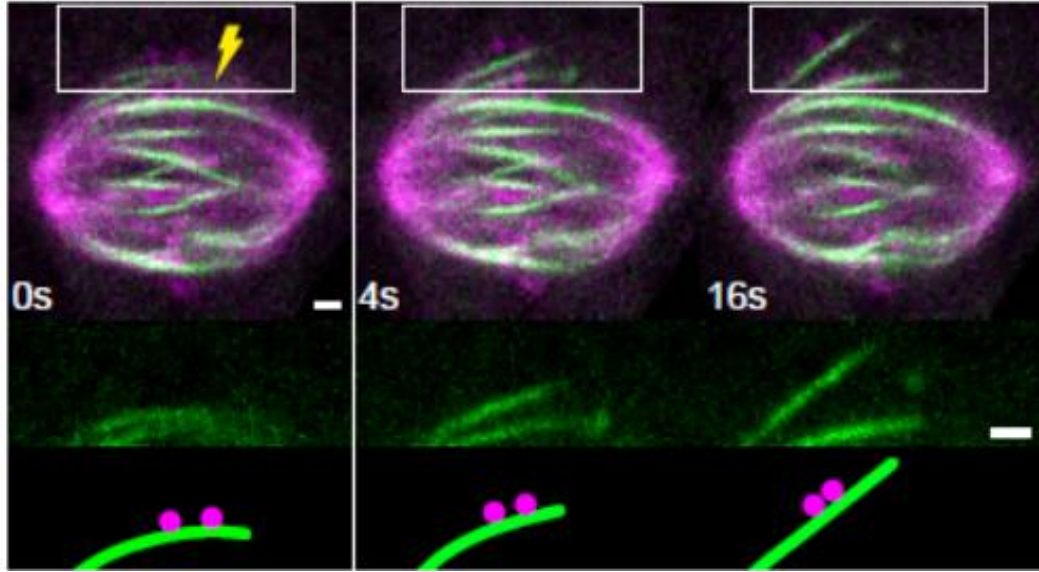


Figure 23. Cell line with thicker bridging fiber have greater response to ablation. Images and illustrations of the HeLa cell expressing PRC1-GFP (green), tubulin mCherry and mRFP-CENP-B (both in magenta). Time-lapse of the mitotic spindle in merged channels showing strong reaction of spindle element to ablation (top left panel). Time-lapse of the mitotic spindle in PRC1-GFP channel showing strong reaction of spindle element to ablation (middle left panel), illustration of the model of presented live images (bottom left panel).

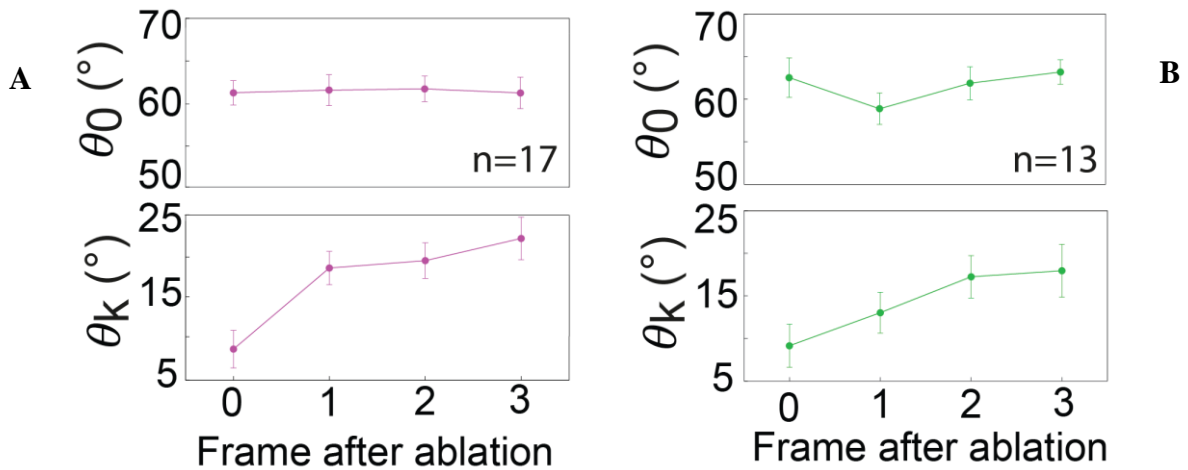


Figure 24. Quantification of response to laser ablation in cells with thicker bridging fiber. A) The angles θ_p and θ_k as a function of frame after laser ablation in HeLa cells expressing PRC1-GFP, mCherry-tubulin and mRFP-CENP-B. B) The angles θ_p and θ_k as a function of frame after laser ablation in the HeLa cell line transiently expressing CENP-Q-GFP and mCherry-tubulin.

4 Discussion

4.1. Bridging microtubules in new force map of the spindle

As I described in introduction, force map of the metaphase spindle that was accepted for a long time in the field, assuming tensed k-fiber along their length, cannot explain some important experimental data and thus is not satisfactory any more. We can argue that much is known about molecular origin of the forces in the spindle (microtubule dynamics and molecular motors) and many players have been described and analysed to date in numerous *in vitro* experiments, but integration of that molecular knowledge into a mesoscopic molecular force model of the spindle is a new objective in studies of spindle mechanics. In excellent reviews, Dumont and Mitchison (2009) and Dumont and Mitchison (2012), have proposed new force map in which they integrated results from many different experiments, including molecular and mechanical perturbation of different spindle elements (Figure 25). They tried to answer some basic mechanical questions using biophysical approach in which molecular interactions and different proteins are abstracted into intrinsically mechanical structures. The simplest question is description of structures that are under tension, and those that are compressed in the spindle. Revised model proposes that k-fibers are under tension near kinetochores and under compression near the poles (Figure 25). Tension that is generated at metaphase chromosomes must be balanced by compression in another spindle element. It was proposed that some hypothetical non-microtubular structure, termed 'spindle matrix', must be present from pole to pole and that this structure is balancing forces generated at kinetochores. To do so, this element must make mechanical interactions with k-fiber along its length so these structures together can oppose forces at kinetochores. To date, several candidates for this function have been proposed.

One candidate is NuMa (nuclear mitotic apparatus) protein, which accumulates mostly at spindle poles at mitosis and is involved in tethering and stabilisation of microtubule minus-ends at spindle poles and in focussing microtubules at spindle poles independently of centrosomes (Radulescu and Cleveland, 2009). It is believed it is main component of spindle pole matrix into which most of the spindle microtubules are tethered. Another candidate is Skeletor, chromosomal protein that forms macromolecular complex with other nuclear components at mitosis and is believed to form structural support in spindle matrix that can anchor motor molecules during force production and microtubule sliding. It was also shown

that this protein localisation is similar in shape with microtubular spindle during mitosis as it precedes assembly of microtubule spindle formation (Walker, 2000). Last component proposed to date is poly(ADP-ribose) (PAR), large, branched, negatively charged polymer whose polymerisation onto acceptor molecules is catalysed by a family of poly(ADP-ribose) polymerases (PARPs) (Chang, 2004). It is enriched at kinetochores and at spindle poles and it is known as component required for maintenance of bipolar spindle structure. Spindle matrix hypothesis proposes that components or their complexes that are separate from spindle microtubules, collectively termed spindle matrix, can contribute to force generation in the spindle and make some interactions with microtubular spindle elements (Pickett-Heaps et al., 1997). In addition, besides components within spindle, some propose that a candidate element may lie outside the spindle. Main candidate is endoplasmic reticulum membrane system that enclose spindle in some system and can contain residue of the interphase nuclear envelope (Dumont and Mitchison, 2012). Main problem with all this hypotheses, in light of our previous reasoning, is that none of these has been shown to stretch continuously from pole to pole making contact with k-fiber and acting as elastic element.



Figure 25. New force map of metaphase spindle. Old tensed k-fibers force map (left) and revised force map that introduces both compression and tension within k-fiber (right) (Adapted from Dumont and Mitchison, 2012).

In contrast to this, our group has proposed non-kinetochore microtubular mechanical element that stretches between poles and can oppose forces generated at kinetochores. We hypothesized that this microtubular structure is composed of antiparallel microtubules and it bridges the gap between kinetochores while interacting laterally with sister k-fibers along most of their length so we named it bridging fiber (Figure 24). Similar non-kinetochore microtubular structures were previously observed using electron microscopy in different systems (Jensen, 1982), (McDonald et al., 1992), but their precise structure and function were not explained. This microtubular structure can explain mechanical paradox that was generated from recent

experimental data (reviewed in introduction) in which one spindle element withstands both tensile forces at kinetochores and compressive forces in region closest to pole. This is paradoxical because k-fiber is largely inextensible, solid rod-like structure (Dumont and Mithison, 2012). My results from pure imaging confirm presence of such structure between sister kinetochores on outermost spindle elements, both in Ptk1 and different HeLa cell lines. This structure would represent new subpopulation of non-kinetochore microtubules within spindles of mammalian cells. Although both microtubules form mainly antiparallel bundles, main difference is lateral interactions of bMT fibers with k-fibers along their length. This interaction enables bMT fiber to influence forces that act on k-fibers, as I have shown above. Nature of this interaction in molecular detail, involving proteins mediating interaction, requires further study, but in present these interactions were abstracted at mesoscopic scale.

To better characterize this microtubular structure I measured its thickness in different cell lines by measuring relative intensity in given regions. Measured thickness would enable us to, not just estimate number of MT in bMT fiber, but also to calculate bMT stiffness that is in theoretical model of the mitotic spindle (see next section) in direct relation with thickness. Measured thicknesses are in agreement with previous observation of thicknesses of MTs laterally connected with k-fibers, both in Ptk1 (Dong et al., 2007) and HeLa cell line (Kajtez, 2014). The observed difference in bMT thickness in Ptk1 and HeLa cell lines may reflect difference in general shape of the spindle that was also shown in our analysis (Table 1). This difference in shape suggests difference in force balance mechanisms in these spindles that must accommodate this shape in dynamic steady state in mitosis, together with other differences in mechanical properties of those cells and HeLa spindles are generally more rounded with more curved outermost spindle element, while in Ptk1 cells spindles are more elongated with more straight outermost spindle elements. This can be seen from our results (Table 1) where spindles in Ptk1 are generally more elongated but narrower than those in HeLa cells. Different thicknesses of bMT fibers indicate different force balance mechanisms in these spindles that reflect itself in different shapes I observed for each cell line I studied. Proposed antiparallel nature of bridging bundles, although not direct objective of this study, was confirmed from observed localisation of PRC1 protein in midzone of spindle element between sister kinetochores of metaphase spindles of HeLa cells expressing PRC1-GFP, tubulin mCherry and mRFP-CENP-B (Figure 21). Explanations that are more detailed can be seen elsewhere (Solomatina, 2014). In addition, thicker bMT fibers in these cells were expected because they are constructed to simultaneously overexpress tubulin and PRC1 crosslinking protein

(Solomatina, 2014). Higher tubulin levels would increase spindle microtubule formation and higher PRC1 levels would increase binding rate of this protein to antiparallel microtubules in antiparallel fibers, such as bMT fiber.

4.2. Spindle element is a single mechanical unit under both compression and tension forces

Describing position of bridging fiber between sister kinetochores and its thickness cannot explain role of this structure in force-balance of metaphase spindles. I defined spindle element as single structural unit comprised of sister k-fibers linked with their kinetochores and connected to a bridging fiber. That definition assumes lateral connections between bMT fiber and sister k-fibers. To probe the nature of forces and existence of such lateral connections acting on k-fibers I analysed videos of HeLa and Ptk1 cell lines where laser ablation was performed. I confirmed that this spindle element, defined mainly by lateral interactions between sister k-fibers and bMT, behave as single mechanical unit following laser ablation. This can be seen from collective outward (away from the line connecting spindle poles) movement of kinetochore pairs, intact k-fiber, bMT fiber and ablated k-fiber stub, both in HeLa and Ptk1 cell lines. This also suggests that these lateral interactions are strong enough to withstand strong physical perturbation, such is ablation of k-fiber(s). To conclude, results confirm that bridging microtubules are part of a spindle element laterally connected with sister k-fibers and that k-fibers are under compression forces that force them to bend.

To better analyse velocity of straightening of spindle element, which I observed after ablation, I used data acquired from tracking of outermost k-fibers at one frame before, and three frames after ablation in HeLa and Ptk1 cell lines. It was crucial to define velocity of straightening in cell lines of different bMT thickness because I hypothesized that cell lines with thicker bMT fibers show faster straightening because of larger force release at the bMT fiber after ablation. Straightening can be seen from increase in pole-KC-KC angle in all cell lines studied and increase in angle at the kinetochore (θ_k) in all HeLa cell lines studied. The two findings together in HeLa cells show us that the spindle element became straighter after the cutting, which is consistent with the observed aligning of the k-fiber stub with the intact k-fiber in HeLa cell lines (Kajtez, 2014) (Figure 15). Perplexing behaviour in Ptk1 cell line can be explained by imprecise nature of measurements in those cell line where resolution at pixel size it not so good as in other videos, which can, together with delicate changes in shape of spindle

element, create perplexing measurements. The largest increase of this angle observed in cell line with thickest bMT fibers suggests that our hypothesis was correct and there is correlation between number of MTs in bridging fiber and velocity of straightening of outermost spindle element. Therefore, I can conclude that, as expected, the spindle element straightened faster in these cells with thicker bridging fibers than in original HeLa tub-GFP and Ptk1 cell lines. Consistent with these results, I observed that the k-fiber stub became more aligned with the intact k-fiber in cells with thicker bridging fibers. It can be concluded that the force at the spindle pole and consequently in the bMT fiber increases with the bMT fiber thickness, and I saw that as stronger response to ablation measured in velocity of spindle element straightening.

The inconsistent behaviour in HeLa cell line transiently expressing CENP-Q-GFP and mCherry-tubulin can be result of strict definition of geometric parameters, which encompassed just some movements of spindle element that can be correlated with bridging fiber thickness. However, it is more likely that measuring of bridging fiber thickness was probably imprecise in some manner in this cell line, probably overestimating bridging fiber thickness. This is not surprising because resolution of these videos was not adequate which together with low cell number of analysed cells caused observed inconsistency in our results. In addition, similar bMT fiber thickness in HeLa cell line transiently expressing CENP-Q-GFP with mCherry-tubulin and HeLa cell expressing PRC1-GFP and tubulin-mCherry indicates that thicker bMT fiber is the result of overexpression of tubulin linked with mCherry, as this is characteristic shared by both cell lines. It is unclear why mCherry, a commonly used fluorophore, would cause appearance of thicker bridging fibers, but I can reason that maybe these cell lines have different expression levels of PRC1 protein instead. That assumption would require future measurements that were not part of this study. Furthermore, because of resolution limits of microscopy systems used and weak mCherry-tubulin signal in all cell lines where this fluorophore was used, I were forced to use small number of cells that are suitable for this analysis (see Materials and methods), and this small numbers surely limit strength of our deduction. Further work, including analysing protein expression levels in individual and population of HeLa cells, is clearly required to define whether thicker bridging fiber is result of PRC1 overexpression or overexpression of mCherry tubulin. In addition, straightening together with outward movement of k-fiber suggests that compressive forces are active along the outermost k-fiber in our spindles. Some other studies have also shown that k-fibers are under compression. For example, UV-microbeam severing of multiple inner k-fibers resulted in bending of intact k-fibers and shortening of the half-spindle length (Pickett-Heaps et al., 1997). Furthermore, treatment of

Xenopus egg extracts with microtubule-depolymerizing drug resulted in bending of intact k-fibers, reduction in kinetochore tension and shortening of the spindle (Mitchison et al., 2005). The possible mechanisms governing the sources of this compression forces that act along k-fibers represent the same mechanisms that govern the spindle length regulation. Main candidate for this role is antagonistic sliding filament mechanism that exerts forces through sliding of array of antiparallel microtubules by motor proteins (Goshima and Scholey, 2010). This antiparallel sliding of ipMTs that are cross-linked in antiparallel orientation in the central region of the spindle is main mechanisms for length regulation, at least in some, but not in all mitotic spindles. Compression could be generated by activity of minus-end directed motor proteins (e.g. homodimeric kinesin-14 and/or dynein) that slide ipMTs and in doing so, they are increasing the overlapping region of ipMTs and decreasing pole-to-pole distance. This would result in production of great inward force if there were no much opposition from plus-end directed proteins doing opposite work in producing outward force on the poles. This was shown by recent experiments in which codepletion of dynein antagonists plus-end directed motors Eg5 and Kif15 resulted in excessive inward force in the spindle. This result suggests that Eg5 and Kif15 generate an outward-directed force on the spindle poles and this force is counterbalanced by inward-directed force generated by dynein (van Heesbeen et al., 2014). This antagonistic outward and inward forces must be tightly regulated (e.g. force-balanced) for proper control of spindle assembly and eventually for forming of correct KT-MT attachments and normal chromosome segregation. Other mechanisms that can influence spindle length and contribute to generation of compression on k-fiber include tight balance of microtubule polymerisation-depolymerisation dynamics (e.g. poleward flux) and microtubule sliding mechanisms described above. Rate of ipMT minus-end depolymerisation at spindle poles can control the rate and extent of spindle elongation due to forces that are exerted on spindle poles by outward-sliding of ipMTs, in that way controlling spindle length and consequently forces acting on spindle element (Goshima and Scholey, 2010). In addition, astral forces generated from astral microtubules pushing on cell cortex can control spindle length. When growing astral MTs from centrosomes at different cell sides hit the cell cortex, they can develop compressive force via a polymerisation mechanism that is directed toward the cortex. This in turn produces an inward force on centrosomes that decrease the pole-to-pole distance. This was shown for some model systems, including movement of interphase nuclei and anaphase spindle in fission yeast (Tolic-Norrelykke et al. 2004, Tran et al. 2001), but not for metaphase spindles in mammalian cells. This pushing force produced by astral microtubules is counterbalanced by pulling force produced when cortical dynein captures astral microtubules and walks toward their minus-end

while it is anchored at cell cortex. This produces pulling force on spindle poles and this balance between pulling and pushing on astral microtubules is very important mechanism of spindle positioning (Rosenthal, 2013). Further research in this field will provide more insights about compression-producing mechanism in metaphase spindles of mammalian cells and function of bMT fibers in that force production, especially in poleward flux of k-fibers.

I also confirmed that kinetochores are under tension that pulls kinetochores from each other (e.g. they experience pulling forces), in Ptk1 metaphase spindles. Resolution of that force by laser ablation resulted in dramatic drop in inter-kinetochore distance. I observed that following spindle element ablation sister kinetochores moved toward each other, in other words, in most Ptk1 cells I observed strong decrease in inter-kinetochore distance. This is in agreement with previous studies studying and confirming tension on metaphase kinetochores by depolymerisation agents such as nocodazole (Waters et al., 1996), or by ablation of one of the kinetochores (McNeill and Berns, 1981), both resulting in reduction of tension between kinetochores. Similar decrease in inter-kinetochore distance was also reported after laser ablation assays similar to ours (Elting et al., 2014, Sikirzhyski et al., 2014). These pulling forces are thought to be generated primarily at the interface of kinetochores and microtubule plus-ends by microtubule depolymerisation (discussed above) or by activity of minus-end directed motors, such as dynein. There is possibility that depolymerisation or activity of plus-directed motors at minus-ends can generate tension at kinetochores, but this theoretical possibility was never observed experimentally (Dumont and Mitchison, 2012). This tension between sister kinetochores is crucial for passage through spindle assembly checkpoint (SAC) pathway because kinetochores with insufficient or no tension at all are quickly destabilized at interface with microtubules. Destabilisation is performed by phosphorylation of microtubule-binding proteins in the kinetochore complex by Aurora B kinase (Lodish et al., 2014). Interestingly, I observed correlation between position of the cut and degree of reduction of inter-kinetochore distance in Ptk1 cells. That was in agreement with studies in our lab done on same HeLa cells expressing tubulin-GFP and CENPB-RFP (Kajtez, 2014). In HeLa cells, it was estimated that junction point along k-fiber where k-fiber and bMT fiber meet is positioned around 1 μm from the kinetochore because all cuts at distance shorter than that does not result in a significant decrease in inter-kinetochore distance, in contrast with cuts longer than that (Kajtez, 2014). I observed same sharp transition at approximately 1.25 μm from kinetochore. Some analogous findings were observed after laser ablation of a k-fiber a few μm away from the kinetochore in *Drosophila* S2 cells and newt epithelial cells where kinetochores

generally do not oscillate (Pickett-Heaps et al., 1997, Maiato et al., 2004). They interpreted this results as indication that kinetochores are locked in N-state in these systems, where there is no active production across the centromere. These experiments also suggest that tension at the kinetochore is balanced by poleward forces exerted on first few of the k-fiber (Dumont and Mitchison, 2012). All these results, including our own, can be explained by our model of mitotic spindle that include bridging fiber. Our results also indicate that junction point is located around region of 1 μm from kinetochores in HeLa cells, and around 1.25 μm from kinetochore in Ptk1 cells. These results also indicate that tension force that acts on sister kinetochores is greatly reduced as we pass this region where junction point is located which would suggest that bMT fiber is important element in force-balance at interface of kinetochores with sister k-fibers.

In conclusion, I have shown that both compression and tension, as antagonistic forces, coexist in single spindle element. It is important to emphasize that this already proposed model (Dumont and Mitchison, 2009) was not explained to date by some mechanical model that comprises all experimental requirements. I can conclude that this new microtubular structure and model it encompasses can explain this mechanical paradox in which one spindle element, which is largely inextensible, solid rod-like structure, withstands both tensile forces at kinetochores and compressive forces in regions closer to spindle pole.

4.3. Theoretical model of spindle element and future prospects

To better define positions where compression and tension forces act and to estimate their values, theoretical model of the HeLa metaphase spindle was developed in collaboration with Nenad Pavin group and solved by Maja Novak (Department of Physics, Faculty of Science, University of Zagreb, Zagreb, Croatia). Microtubule fibers in this model are represented as elastic rods taking into account the elastic properties of MT bundles and the forces acting at their ends; there are two k-fibers in the model and one bMT fiber and they merge at two junction points along k-fiber length (Figure 26). K-fibers by one side end on kinetochores that are connected by centromeric heterochromatin that lies between kinetochores and is represented as elastic spring. The tension between sister kinetochores that stretch centromeric region is described as a pulling force acting at the end of the k-fiber that corresponds to the position of the kinetochore (F_k). Other end of k-fiber end near the centrosomes and torque is introduced (M_o) acting on the poles to mimic experimental finding that on the poles spindle element is clamped (it is not freely

joined). Otherwise, it is important to note that the distance between pole is fixed. Other force introduced is compressive force that act on k-fibers from the spindle poles (F_0). The bending rigidity of the k-fiber and the bridging fiber were determined by multiplying the known bending rigidity of a single MT with the number of MTs in the respective fibers that I measured experimentally.

Inputs for solving the model where experimentally measured geometric properties of the HeLa mitotic spindle (Table 1): spindle length and width, angles at the kinetochore and the spindle pole and the measured thickness of the bMT fiber (e.g. estimation of number of microtubules in bMT fiber). Outputs in the model solving were position of the junction point and the forces at the spindle poles and kinetochores. This theoretical model has predictions that are important for analysis of my experimental data: 1. Shape of the mitotic spindle is convex; 2. junction point is positioned $0.75 \mu\text{m}$ away from the kinetochore; 3. kinetochores are above the bridging fiber; 4. force at the spindle pole acts inwards, resulting in the compression and buckling of the bridging fiber; 5. tension at the kinetochore propagates along the segment of the k-fiber between the junction and the kinetochore; 6. two inward forces are counteracted by the compression in the central segment of the bridging fiber between the two junctions.; 7. the thicker bMT fiber is the larger force at the spindle pole is, and consequently a larger is force in the bridging fiber (Kajtez et al., unpublished data).

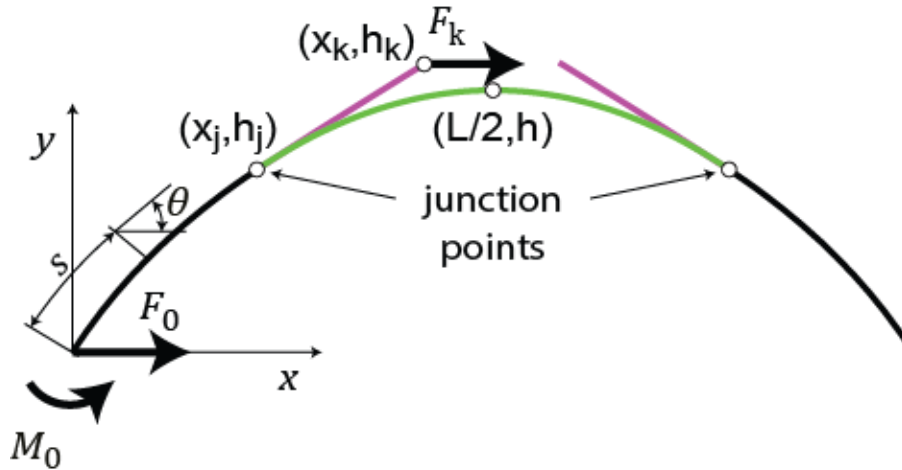


Figure 26. Theoretical model of HeLa cell mitotic spindle. Schematic representation of the theoretical model of HeLa cell metaphase spindle including bMT microtubules developed by Nenad Pavin group and solved by Maja Novak. Black line represent rod extending from the position that represent the spindle pole until the junction point, magenta line represent rod that extends from the junction point to the position that represent kinetochore, and green line represent bridging rod that extends between two junction points. The geometry of each rod is described by a tangential angle, (s), along the contour length, s . Forces at the spindle pole, F_0 , and at the kinetochore, F_k , as well as the torque at the spindle pole, M_0 , are depicted.

Results obtained from solving model equations, after including some of our experimental data, together with well-known constants as inputs, confirmed our experimental observations. Tension forces are found to be acting on segment of k-fiber between the junction and the kinetochore, while the rest of the k-fiber including laterally connected bMT fiber and central region of bMT fiber between the two junction points, are under compression. I reason, that central part of bMT fiber balances the antagonistic forces acting on the poles and at the kinetochores, making this perplexing presence of tension and compression forces within single spindle element possible. Model also have some important predictions that I would mention here because they were used to form hypothesis and plans in this project. First, theoretical model predicts that shape of mitotic spindle is convex, which may seem trivial, but it confirms that parameters, used for calculations in the model solving, are of biological importance, or at least observed in our experiments (Figure 8). Second, model predicts that sister kinetochore pair is positioned above bMT fiber, away from the central axis connecting two spindle poles. This is important because in all our analysed videos of HeLa and Ptk1 cells where I could observe bMT fiber, it was positioned below sister KT pair, toward center of the spindle (Figures 8 and 9). In addition, model predicted that there is correlation between bMT fiber stiffness (directly related to its thickness, e.g. number of MT in fiber) and velocity of straightening and displacement of spindle element after the cut. We tested this hypothesis experimentally and confirmed these predictions (see above). In addition, model predicts that, in HeLa cells metaphase spindle, junction point is positioned $0.75\ \mu\text{m}$ away from the kinetochore. That is in agreement previously observed experimental prediction that junction point is located in region around $1\ \mu\text{m}$ from the kinetochore (Kajtez, 2014). In future, it would be interesting to see what model predicts about metaphase spindle behaviour in Ptk1 cell line, especially role of bMT fiber, because difference in spindle shape and bMT thickness in these cells compared with HeLa cell line, indicate some different force balance mechanisms.

Future work will be required to define role and structural dynamics of bMT fiber in chromosome segregation in anaphase and to better define its role in tension between kinetochores in metaphase and poleward flux in metaphase and anaphase, both in HeLa and Ptk1 cell lines. In light of this, it will be important to define motor proteins and crosslinkers acting between bMT fibers and between k- and bMT fiber, and to what extent sliding between these fibers contributes to processes and mechanisms that are crucial for spindle maintenance and function in metaphase and anaphase. It would be interesting to see what happens with bMT

fiber at metaphase-anaphase transition when dynamic steady state is disturbed. Our present observations indicate that most antiparallel microtubules marked with PRC1-GFP protein are linked with kinetochores, so it would be interesting to analyse how structure of spindle element is withstanding and changing in response to forces acting in anaphase. In addition, causes of thicker bMT fiber in HeLa cell line stably expressing PRC1-GFP and transiently expressing mRFP-CENP-B and mCherry-tubulin are not yet clear, so it would be interesting to define them at molecular level. In theoretical part of project, it would be interesting to create theoretical model for Ptk1 metaphase spindle because our results indicate different force-balance mechanisms in those cells compared with HeLa cells. In addition, we could include motor-driven forces and arrangement of MT polarity and position of their ends in new theoretical model of metaphase spindle and then test experimentally some of the prediction of this dynamic model. All of this would shed more light on structural and functional role of bMT fibers in spindle of different phases of mitosis.

5 Conclusion

In all eukaryotes, segregation of chromosomes is accomplished by formation of highly dynamic macromolecular complex termed mitotic spindle that self-assembles in prometaphase of mitosis. This structure is composed primarily of microtubules and associated proteins. Current models of mitotic spindle recognize three distinct subpopulations of microtubules: kinetochore, interpolar and astral microtubules. Although much is known about origin of forces on molecular scale encompassing molecular motors and microtubule dynamics, integration of those forces on mesoscopic scale is currently one of the main goals in the field. We have approached this problem by formulating a new model of mitotic spindle that includes microtubular structure that spans the region under sister kinetochores and is laterally connected to sister k-fibers. We called this structure bridging microtubule (bMT) that tends to form a bundle of antiparallel microtubules termed bMT fiber. Main goal of this study was to define first architectural and then role in force-balance of bMT in metaphase of mitosis. I observed bMT fibers close below the outermost kinetochore pairs both in HeLa cells expressing tubulin-GFP and CENP-B-RFP and in Ptk1 cells expressing Hec1-GFP and were in addition were injected with X-rhodamine-tubulin. I also measured thickness of bMT fibers to define number of microtubules in bMT fiber in different cell lines. To define role of bMT fibers in force-balance and their lateral attachment to k-fibers in Ptk1 cells, I analysed videos where laser ablation of outermost k-fiber was performed. I observed outward movement of sister kinetochores, intact k-fiber, k-fiber stub and bMT fiber that was directed from central spindle plane. I conclude from the analysis that bMT fibers are laterally connected to sister k-fibers and they constitute single mechanical unit. In addition, I observed strong decrease in inter-kinetochore distance after ablation that was correlated with position of the cut in such a way that I observed strong transition in degree of relaxation in region around $1.25\ \mu\text{m}$ from kinetochore. I concluded, in agreement with previous studies, that tension forces are acting on sister kinetochores. I also quantitatively analysed spindle shape in steady state and after ablation. I showed that velocity of straightening is largest in cell line with thickest bMT fiber and that straightening can be quantitatively described in other cell lines studied. This result confirms that compressive forces are active along spindle element. Finally, I compared our experimental data with theoretical model of the HeLa cell spindle to verify robustness of theoretic model and analyse how predictions of the model fit in our experimental observations. I conclude that bMT fiber is important structural element that balances compressive and tensile forces acting on spindle element in metaphase of mitosis in HeLa and Ptk1 cells.

References

- Aubin J.E., Osborn M., Franke W.W., Weber K. (1980): Intermediate filaments of the vimentin-type and the cytokeratin-type are distributed differently during mitosis. *Exp. Cell. Res.* **129**(1): 149-65
- Alberts B. et al. (2010): Essential cell biology, 3rd ed., Garland Science, New York.
- Bieling P., Telley I.A., Surrey T. (2010): A minimal midzone protein module controls formation and length of antiparallel microtubule overlaps. *Cell* **142**: 420-432
- Bloom, K. S., Joglekar, A. P., Bouck, D. C. (2008): Design Features of a Mitotic Spindle: Balancing Tension and Compression at a Single Microtubule Kinetochore Interface in Budding Yeast. *Annu. Rev. Genet.* **42**: 335–59
- Braun M., Drummond D.R., Cross R.A., McAinsh A.D. (2009): The kinesin-14 Klp2 organizes microtubules into parallel bundles by an ATP-dependent sorting mechanism. *Nat. Cell Biol.* **11**: 724–755
- Brinkley B.R., Stubblefield E. (1966): The fine structure of the kinetochore of a mammalian cell in vitro. *Chromosoma* **19**: 28–43
- Cai S., Weaver L.N., Ems-McClung S.C., Walczak C.E. (2009): Kinesin-14 Family Proteins HSET/XCTK2 Control Spindle Length by Cross-Linking and Sliding Microtubules. *Mol. Biol. Cell* **20**: 1348–1359
- Caudron M., Bunt G., Bastiaens P., Karsenti E. (2005): Spatial coordination of spindle assembly by chromosome-mediated signaling gradients. *Science* **309**: 1373-1376
- Chang P., Jacobson M.K., Mitchinson T.J. (2004): Poly(ADP-ribose) is required for spindle assembly and structure. *Nature* **432**: 645-649
- Cheeseman I.M., Desai A. (2008): Molecular architecture of the kinetochore-microtubule interface. *Nat. Rev. Mol. Cell. Biol.* **9**(1): 33-46
- Civelekoglu-Scholey G., Scholey J.M. (2010): Mitotic force generators and chromosome segregation. *Cell. Mol. Life. Sci.* **67**(13): 2231-2250
- Cross R.A., McAinsh A. (2014): Prime movers: the mechanochemistry of mitotic kinesins. *Nat. Rev. Mol. Cell. Biol.* **15**: 257–271
- Desai A., Mitchison T.J. (1997): Microtubule polymerisation dynamics. *Ann. Rev. Dev. Biol.* **13**: 83–117
- Dogterom M., Recouvreux P. (2012): Dissecting Spindle Architecture with a Laser. *Cell* **149**: 507-509
- Dong Y., Vanden Beldt K.J., Meng X., Khodjakov A., McEwen B.F. (2007): The outer plate in vertebrate kinetochores is a flexible network with multiple microtubule interactions. *Nat. Cell Biol.* **9**: 516-522
- Downing K.H., Nogales E., (1998): Tubulin and microtubule structure. *Curr. Opin. Cell Biol.* **10**: 16–22

- Drechsler H., McHugh T., Singleton M.R., Carter N.J., McAinsh A.D. (2014): The Kinesin-12 Kif15 is a processive track-switching tetramer. *eLife* **3**: e01724
- Dumont S., Mitchison T.J. (2009): Force and Length in the Mitotic Spindle. *Curr. Biol.* **19**: 749-761
- Dumont S., Mitchison T. J. (2012): Mechanical Forces in Mitosis. In: Egelman E. H. (edit.) Comprehensive Biophysics, 4th ed., Molecular Motors and Motility. Oxford: Academic Press. 298-320
- Elting M.W., Hueschen C.L., Udy D.B., Dumont S. (2014): Force on spindle microtubule minus-ends moves chromosomes. *J. Cell Biol.* **206**: 245-256
- Fink G., Hajdo L., Skowronek K.J., Reuther C., Kasprzak A.A., Diez S. (2009): The mitotic kinesin-14 Ncd drives directional microtubule-microtubule sliding. *Nat. Cell Biol.* **11**: 717-723
- Fisher H.K., Deane C.M., Wakefield G.J. (2008): The functional domain grouping of microtubule associated proteins. *Commun Integr Biol* **1**(1): 47-50
- Goshima G., Mayer M., Zhang N., Stuurman N., Vale, R.D. (2008): Augmin: a protein complex required for centrosome-independent microtubule generation within the spindle. *J. Cell Biol.* **181**: 421-429
- Goshima G., Scholey J.M. (2010): Control of Mitotic Spindle Length. *Annu. Rev. Cell Dev. Biol.* **26**: 21-57
- Lu M.S., Johnston C.A. (2013): Molecular pathways regulating mitotic spindle orientation in animal cells. *Development.* **140**(9): 1843-56
- Helmke J. K., Heald H., Wilbur D.J. (2013): Interplay Between Spindle Architecture and Function. In: Kwang W. Jeon (edit.) International Review of Cell and Molecular Biology Volume **306**, Pages 83-125
- Hochegger H., Takeda S., Hunt T. (2008): Cyclin-dependent kinases and cell-cycle transitions: does one fit all? *Nat. Rev. Mol. Cell Biol.* **9**(11): 910-6
- Howard J., Hyman A.A. (2009): Growth, fluctuation and switching at microtubule plus-ends. *Nat. Rev. Mol. Cell Biol.* **10**(8): 569-74
- Hsia K.C., Wilson-Kubalek E.M., Dottore A., Hao Q., Tsai K.L., Forth S., Shimamoto Y., Milligan R.A., Kapoor T.M. (2014): Reconstitution of the augmin complex provides insights into its architecture and function. *Nat. Cell Biol.* **16**(9): 852-63
- Inoue S., Sato H. (1967): Cell motility by labile association of molecules. The nature of mitotic spindle fibers and their role in chromosome movement. *J. Gen. Physiol.* **50**: 259-292
- Jaqaman K., King E.M., Amaro A.C., Winter J.R., Dorn J.F., Elliott H.L., Mchedlishvili N., McClelland S.E., Porter I.M., Posch M., Toso A., Danuser G., McAinsh A.D., Meraldi P., Swedlow J.R. (2010): Kinetochore alignment within the metaphase plate is regulated by centromere stiffness and microtubule depolymerases. *J. Cell Biol.* **188**(5): 665-679
- Jensen, C.G. (1982): Dynamics of spindle microtubule organisation: kinetochore fiber microtubules of plant endosperm. *J. Cell Biol.* **92**: 540-558

- Kajtez J. (2014): Study of Forces in HeLa Cell Metaphase Spindle Using Laser Ablation, Master's thesis, Technische Universität Dresden Biotechnology Center (BIOTEC), Katholieke Universiteit Leuven
- Kitamura E., Tanaka K., Komoto S., Kitamura Y., Antony C., Tanaka U.T. (2010): Kinetochore Generate Microtubules with Distal Plus-ends: Their Roles and Limited Lifetime in Mitosis. *Dev. Cell* **18**(2): 248–259
- Kalinina I., Nandi A., Delivani P., Chacon M.R., Klemm A.H., Ramunno-Johnson D., Krull A., Lindner B., Pavin N., Tolic-Nørrelykke I.M. (2013): Pivoting of microtubules around the spindle pole accelerates kinetochore capture. *Nat. Cell Biol.* **15**(1): 82–87
- Krull A., Steinborn A., Ananthanarayanan A., Ramunno-Johnson D., Petersohn U., Tolic-Norrelykke I. M. (2014.): A divide and conquer strategy for the maximum likelihood localisation of low intensity objects. *Opt. Express* **22**(1): 210-228
- Lodish H. et al. (2014): Molecular cell biology, 7th ed., W. H. Freeman and Company, New York
- Maiato H., Rieder C.L., Khodyakov A. (2004): Kinetochore-driven formation of kinetochore fibers contributes to spindle assembly during animal mitosis. *J. Cell Biol.* **167**(5): 831-840
- Mazumdar M., Misteli T. (2005): Chromokinesins: multitasking players in mitosis. *Trends Cell Biol.* **15**(7): 349-55
- McDonald K.L., O'Toole E.T., Mastroratte D.N., McIntosh J.R. (1992): Kinetochore microtubules in PTK cells. *J. Cell Biol.* **118**: 369–383
- McEwen B.F., Heagle A.B., Cassels G.O., Buttle K.F., Rieder C.L. (1997): Kinetochore fiber maturation in PtK1 cells and its implications for the mechanisms of chromosome congression and anaphase onset. *J. Cell Biol.* **137**: 1567-1580
- McEwen B.F., Chan G.K., Zubrowski B., Savoian M.S., Sauer M.T., Yen T.J. (2001): CENP-E is essential for reliable bioriented spindle attachment, but chromosome alignment can be achieved via redundant mechanisms in mammalian cells. *Mol. Biol. Cell* **12**: 2776-2789
- McIntosh R. J., Molodtsov M. I., Ataullakhanov F. I. (2012): Biophysics of mitosis. *Q. Rev. Biophys.* **45**: 147-207
- McNeill P.A., Berns M.W. (1981): Chromosome behavior after laser microirradiation of a single kinetochore in mitotic PtK2 cells. *J. Cell Biol.* **88**: 543–553
- Mitchison T., Kirschner M. (1984): Dynamic instability of microtubule growth. *Nature* **312**: 237–242
- Mitchison T.J., Evans L., Schulze E., Kirschner M. (1986): Sites of microtubule assembly and disassembly in the mitotic spindle. *Cell* **45**: 515–527
- Mitchison T.J., Maddox P., Gaetz J., Groen A.C., Shirazu M., Desai A., Salmon E.D., Kapoor T.M. (2005): Roles of polymerisation dynamics, opposed motors, and a tensile element in governing the length of *Xenopus* extract meiotic spindles. *Mol. Biol. Cell* **16**: 3064–3076
- Mogilner A., Craig E. (2010): Towards a quantitative understanding of mitotic spindle assembly and mechanics. *J. Cell Sci.* **123**:3435-45
- Mohri H. (1968): Amino-acid composition of 'Tubulin' constituting microtubules of sperm flagella. *Nature* **217**: 1053–1054

- Nicklas R.B., Kubai D.F., Hays T.S. (1982) Spindle microtubules and their mechanical associations after micromanipulation in anaphase. *J. Cell Biol.* **95**: 91–104
- Nogales E., Alushin G. (2012): Tubulin and Microtubule Structure: Mechanistic Insights into Dynamic Instability and Its Biological Relevance. In: Egelman E. H. (edit.) *Comprehensive Biophysics*, 4th ed., Molecular Motors and Motility. Oxford: Academic Press. 298-320
- O’Connell C. B., Khodjakov A.L. (2007): Cooperative mechanisms of mitotic spindle formation. *J. Cell Sci.* **120**: 1717-1722
- Paul R., Wollman R., Silkworth W.T., Nardi I.K., Cimini D., Mogilner A. (2009): Computer simulations predict that chromosome movements and rotations accelerate mitotic spindle assembly without compromising accuracy. *Proc. Natl. Acad. Sci. U.S.A.* **106**(37): 15708–15713
- Pavin N., Tolić-Nørrelykke I.M. (2014): Swinging a sword: how microtubules search for their targets. *Syst. Synth. Biol.* **8**(3): 179-186
- Paweletz N. (2001): Walther Flemming: Pioneer of Mitosis Research. *Nat. Rev. Mol. Cell Biol.* **2**(1): 72-75
- Peterman E.J.G., Scholey M.J. (2009): Mitotic microtubule crosslinkers: Insights from mechanistic studies. *Curr. Biol.* **19**(23): 1089-1094
- Pickett-Heaps J.D., Forer A., Spurck T. (1997): Traction fiber: toward a ‘tensegral’ model of the spindle. *Cell Motil. Cytoskeleton* **37**: 1–6
- Piehl M., Tulu U.S., Wadsworth P. and Cassimeris L. (2004): Centrosome maturation: measurement of microtubule nucleation throughout the cell cycle by using GFP-tagged EB1. *Proc. Natl. Acad. Sci. U.S.A.* **101**: 1584-1588
- Radulescu E.E., Cleveland D.W. (2010): NuMA after 30 years: the Matrix Revisited. *Trends Cell Biol.* **20**(4): 214–222
- Rieder C.L. (1981): The structure of the cold-stable kinetochore fiber in metaphase PtK1 cells. *Chromosoma* **84**(1): 145-58
- Rieder C.L., Salmon E.L. (1994): Motile kinetochores and polar ejection forces dictate chromosome position on the vertebrate mitotic spindle. *J. Cell Biol.*, **124**(3): 223-233
- Rieder C.L., Khodjakov A. (2003): Mitosis through the microscope: Advances in seeing inside live dividing cells. *Science* **300**(5616): 91-96
- Rogers, G.C., Rogers S.L., Sharp D.J. (2005): Spindle microtubules in flux. *J. Cell Sci.* **118**: 1105–1116
- Rüdiger J. (2014): Forces acting on kinetochores during metaphase in PtK1 cells, Master’s Thesis, Technische Universität Dresden
- Shimamoto Y., Maeda Y.T., Ishiwata S., Libchaber A.J., Kapoor M.T. (2011): Insights into the micromechanical properties of the metaphase spindle. *Cell* **145**(7): 1062-1074
- Sikirzhyski V., Magidson V., Steinman J.B., He J., Le Berre M., Tikhonenko I., Ault J.G., N McEwen B.F., Chen J.K., Sui H., et al. (2014). Direct kinetochore-spindle pole connections are not required for chromosome segregation. *J. Cell Biol.* **206**: 231-243

- Solomatina A. (2014): Force Balance in the Mitotic Spindle of Hela Cells Studied by High-Speed Live-Cell Imaging, Master's Thesis, Technische Universitat Dresden Biotechnology Center (BIOTEC)
- Tanaka T.U. (2010): Kinetochore-microtubule interactions: steps-toward bi-orientation. *EMBO J.* **29**: 4070-4082
- Tolić-Nørrelykke I.M., Sacconi L., Thon G., Pavone F.S. (2004): Positioning and elongation of the fission yeast spindle by microtubule-based pushing. *Curr. Biol.* **14**: 1181–86
- Tran P.T., Marsh L., Doye V., Inoue S., Chang F. (2001): A mechanism for nuclear positioning in fission yeast based on microtubule pushing. *J. Cell Biol.* **153**: 397–411
- van Heesbeen R.G., Tanenbaum M.E., Medema R.H. (2014): Balanced activity of three mitotic motors is required for bipolar spindle assembly and chromosome segregation. *Cell Rep.* **8**(4): 948-56
- Walczak C.E., Heald R. (2008): Mechanisms of mitotic spindle assembly and function. *Int. Rev. Cytol.* **265**: 111–158
- Walczak C.E., Cai S., Khodjakov A. (2010): Mechanisms of chromosome behaviour during mitosis. *Nat. Rev. Mol. Cell Biol.* **11**(2): 91–102
- Walker D.L., Wang D., Jin Y., Rath U., Wang Y., Johansen J., Johansen K.M. (2000): Skeletor, a novel chromosomal protein that redistributes during mitosis provides evidence for the formation of a spindle matrix. *J. Cell Biol.* **151**(7): 1401-12
- Wang H., Brust-Mascher I., Scholey J.M. (2014): Sliding filament and spindle organisation. *Nat. Cell Biol.* **16**: 737-739
- Waters J.C., Mitchison T.J., Rieder C.L., Salmon E.D. (1996): The kinetochore microtubule minus-end disassembly associated with poleward flux produces a force that can do work. *Mol. Biol. Cell* **7**: 1547–1558
- Wiese C., Zheng Y. (2006): Microtubule nucleation: gamma-tubulin and beyond. *J. Cell Sci.* **119**: 4143-53
- Wittmann T., Hyman A., Desai A. (2001): The spindle: a dynamic assembly of microtubules and motors. *Nat. Cell Biol.* **3**(1): 28-34
- Yang Z., Tulu U.S., Wadsworth P., Rieder C.L. (2007): Kinetochore dynein is required for chromosome motion and congression independent of the spindle checkpoint. *Curr. Biol.* **17**: 973–980
- Yokoyama H., Gruss O.J., Rybina S., Caudron M., Schelder M., Wilm M., Mattaj J.W., Karsenti E. (2008): Cdk11 is a RanGTP-dependent microtubule stabilisation factor that regulates spindle assembly rate. *J. Cell Biol.* **180**: 867-875

Curriculum vitae

Basic information:

- ❖ Given name: Kruno
- ❖ Family name: Vukušić
- ❖ Date of birth: 12 June 1991
- ❖ Place of birth: Split, 21000, Croatia
- ❖ Address of residence: Put Duilova 4a, 21000, Split, Croatia
- ❖ Address of habitual residence: Trg Francuske Republike 6, 10000, Zagreb, Croatia
- ❖ Nationality: Croatian
- ❖ e-mail: vukusic.kruno@gmail.com

Education:

- ❖ 2006 – 2010: High school Vladimir Nazor, 21000, Split, Croatia. Finished with The state graduation exam.
- ❖ 2010 – 2013: Undergraduate university study programme in biology, University of Zagreb, Faculty of Science, 10000, Zagreb. Finished with bachelor thesis “Mechanisms of B-cell lymphoma development” under supervisorship of Dr. Petra Korać, Assoc. Prof. (Department of Molecular Biology, Division of Biology, Faculty of Science, University of Zagreb, 10000 Zagreb, Croatia). Acquired title Bachelor in Biology (univ. back. biol.).
- ❖ 2013 – to date: Graduate university study programme in molecular biology, University of Zagreb, Faculty of Science, 10000, Zagreb, Croatia.

Awards and Achievements:

- ❖ 2012. Commendation for distinct accomplishments during study from Board of Faculty of Science.

Scholarships:

- ❖ 2011 – 2014: State scholarship from Ministry of Science, Education and Sports for especially talented regular students of university and professional programmes.
- ❖ 2014 – to date: City of Split scholarship for students of undergraduate, graduate and integrated programmes with distinct accomplishments during study.

Attended meetings and conferences:

- ❖ HDIR-3 “From Bench to Clinic”, Third Meeting of the Croatian Association for Cancer Research with International Participation.